Available online at www.sciencedirect.com
ScienceDirect
Planetary and Space Science 58 (2010) 40–60
Planetary and Space Science
www.elsevier.com/locate/pss

The BepiColombo mission: An outstanding tool for investigating the Hermean environment

A. Milillo[a,*], M. Fujimoto[b], E. Kallio[c], S. Kameda[b], F. Leblanc[d,e], Y. Narita[f], G. Cremonese[g], H. Laakso[h], M. Laurenza[a], S. Massetti[a], S. McKenna-Lawlor[i], A. Mura[a], R. Nakamura[j], Y. Omura[k], D.A. Rothery[l], K Seki[m], M. Storini[a], P. Wurz[n], W. Baumjohann[j], E.J. Bunce[o], Y. Kasaba[p], J. Helbert[q], A. Sprague[r], the other Hermean Environment WG members[1]

[a]*INAF/IFSI, Rome, Italy*
[b]*JAXA/ISAS, Japan*
[c]*FMI, Helsinki, Finland*
[d]*Service d'Aeronomie du CNRS, Verrieres Le Buisson, France*
[e]*INAF/OATS, Trieste, Italy*
[f]*IGEP, TU Braunschweig, Germany*
[g]*INAF/OAPD, Padova, Italy*
[h]*ESA, Estec, Holland*
[i]*STIL National University of Ireland, Maynooth, Co. Kildare, Ireland*
[j]*Space Research Institute, Austrian Academy of Sciences, 8042 Graz, Austria*
[k]*Research Institute for Sustainable Humanosphere, Kyoto University, Japan*
[l]*Department of Earth & Environmental Sciences, Open University, Milton Keynes, UK*
[m]*STEL & IAR, Nagoya University, Aichi, Japan*
[n]*Physikalisches Institut, University of Bern, Switzerland*
[o]*Space Research Centre, University of Leicester, UK*
[p]*Department Geophysics, Graduate School of Science, Tohoku University, Japan*
[q]*DLR, Berlin, Germany*
[r]*Lunar and Planetary Laboratory, University of Arizona, Tucson, USA*

Received 20 February 2008; received in revised form 27 May 2008; accepted 5 June 2008
Available online 22 June 2008

Abstract

Mercury possesses a weak, internal, global magnetic field that supports a small magnetosphere populated by charged particles originating from the solar wind, the planet's exosphere and surface layers. Mercury's exosphere is continuously refilled and eroded through a variety of chemical and physical processes acting in the planet's surface and environment. Using simultaneous two-point measurements from two satellites, ESA's future mission BepiColombo will offer an unprecedented opportunity to investigate magnetospheric and exospheric dynamics at Mercury as well as their interactions with solar radiation and interplanetary dust. The expected data will provide important insights into the evolution of a planet in close proximity of a star. Many payload instruments aboard the two spacecraft making up the mission will be completely, or partially, devoted to studying the close environment of the planet as well as the complex processes that govern it. Coordinated measurements by different onboard instruments will permit a wider range of scientific questions to be addressed than those that could be achieved by the individual instruments acting alone. Thus, an important feature of the BepiColombo mission is that simultaneous two-point measurements can be implemented at a location in space other than the Earth. These joint observations are of key importance because many phenomena in Mercury's environment are temporarily and

*Corresponding author. Tel.: +39 06 4993 4387.
E-mail address: anna.milillo@ifsi-roma.inaf.it (A. Milillo).
[1]See Appendix section.

0032-0633/$ - see front matter
doi:10.1016/j.pss.2008.06.005

spatially varying. In the present paper, we focus on some of the exciting scientific goals achievable during the BepiColombo mission through making coordinated observations.

Keywords: Mercury's exosphere; Mercury's magnetosphere; Solar wind–planets interaction

1. Introduction

Previous to 2008, the only space-based information about Mercury came from three flybys performed in 1974–1975 by the Mariner 10 spacecraft. The first flyby on 27 March 1972 was due to an augmentation to its original mission (Vilas et al., 1988). Thereafter, Giuseppe Colombo, a mechanical engineer at the University of Padova, Italy, noted that, after this flyby, Mariner 10 had an orbital period around the Sun that was close to twice Mercury's orbital period. This suggested that a second encounter with the planet could rather easily be accomplished and, having confirmed this possibility, personnel at the Jet Propulsion Laboratory, Pasadena carefully adapted Mercury flight parameters in order to achieve a gravity correction that returned the spacecraft to Mercury some 6 months later (21 September 1972). The final flyby took place on 16 March 1975.

Later Earth-based observations revealed important features about the exosphere of Mercury (see reviews by Killen et al., 2008; Cremonese et al., 2008), but they are limited to species observable from the ground (Na, K and Ca). Nevertheless, the proximity of Mercury to the Sun makes studies of those extreme environmental conditions that led to its unique evolutionary history of particular importance. Mercury's present plasma environment is characterised by a weak internal global magnetic field that supports a small magnetosphere populated with plasma originating from the solar wind and from the planet's exosphere. In fact, Mercury's exosphere is continuously refilled and eroded by interaction processes with the planetary surface, the magnetospheric and solar wind plasma, and solar radiation (Killen and Ip, 1999; Killen et al., 2001; Wurz and Lammer, 2003; Milillo et al., 2005; Leblanc et al., 2007). Investigations of magnetospheric dynamics, the planet's interaction with solar radiation (both electromagnetic and corpuscular) and with interplanetary dust can provide important clues to the process of planetary evolution.

Two missions are presently scheduled to explore the iron planet, namely: NASA's MESSENGER mission (Solomon et al., 2007) that was launched in March 2004 and had its first and second flybys of Mercury in 14 January and 6 October 2008, respectively, and the BepiColombo (BC) mission (Hajakawa et al., 2008; Schulz, 2006), developed jointly by ESA and JAXA, which will be launched in August 2013. These initiatives have stimulated new interest in the many unresolved mysteries related to Mercury.

The observations of the MESSENGER first flyby in the Mercury's nightside indicate that the magnetosphere was found to be similar to that seen by Mariner 10 (Solomon et al., 2001; Gold et al., 2001; Santo et al., 2001). In particular, Na and Ca were observed in the exosphere, H and Na corona forming an anti-sunward tail were imaged and Mg was observed for the first time (McClintock et al., 2008; Killen et al., 2008). Also, heavy ions were measured in the magnetosphere (Zurbuchen et al., 2008; Slavin et al., 2008). The prognosis is good for the other flyby 29 September 2009 before MESSENGER goes into an eccentric orbit in March 2011.

The BC mission is composed of two spacecraft: the Mercury Planetary Orbiter (MPO) and the Mercury Magnetospheric Orbiter (MMO). Each of these spacecraft will be equipped with state-of-art instruments that will provide the most comprehensive measurements available. BC has among its major scientific objectives: (a) determination of the composition, origin and dynamics of Mercury's exosphere and polar deposits and (b) investigation of the structure and dynamics of Mercury's magnetosphere. Many of their instruments are completely, or partially, dedicated to studying the planetary environment and the processes that give rise to it. While each individual instrument is expected to reveal important new information concerning the planet and its environment, inter-instrument collaborations will allow yet further insights to be gained into Hermean circumstances. A further even more special and powerful feature of the BC mission from the environmental research point of view is that two-point simultaneous measurements can be implemented by MPO and MMO. Such measurements are essential to the investigations of Mercury's environment because it varies rapidly both spatially and temporarily (e.g. Baumjohann et al., 2006; Fujimoto et al., 2007, 2008).

In this paper, we briefly review our current understanding of Mercury's environment and present an account of the key scientific investigations concerning Mercury's exosphere and magnetosphere that will be carried out during the BepiColombo mission. This paper thus fulfils the same role as the overview papers of Slavin et al. (2007) and Domingues et al. (2007) that relate to the magnetospheric and exospheric science strategy implemented aboard MESSENGER mission. Section 2 presents our knowledge of the surface–exosphere–magnetosphere system of Mercury. In Section 3, the currently supposed origin and configuration of the Hermean magnetosphere and the nature of key exospheric processes are described. In Section 4, we outline investigations that will be implemented by different instruments of the BC mission through cooperative measurements. In particular, examples of primary scientific goals related to magnetospheric dynamics

achievable with simultaneous two-point measurements (Section 4.1) will be outlined, as well as the goals related to the surface properties of the planet that can be revealed by the investigations of the environment (Section 4.2).

2. Magnetosphere–exosphere–upper surface of Mercury from observations

The Mariner 10 flybys revealed that Mercury has an intrinsic global magnetic field that gives rise to a small magnetosphere, bounded by a magnetopause, and a bow shock (for a review, see Russell et al., 1988; Wurz and Blomberg, 2001; Slavin et al., 2007). The in situ data showed that this magnetic field is relatively weak; therefore, the Hermean magnetopause is located close to the planetary surface. The estimated magnetopause–planetocentric distance is about 1.7 planetary radii (compare with 10 planetary radii in the case of the Earth's magnetosphere). Nevertheless, at 0.3 AU, large variations in magnetopause location in response to solar wind pressure fluctuations are expected. Mercury features a "miniature" magnetosphere, whose linear dimensions are about 5% those of the Earth (Russell et al., 1988). It is indeed so small that the gyroradii of energetic protons and heavier ions are comparable to the dimensions of this magnetosphere and thus, when modelling particle trajectories, the guiding centre approximation is not applicable.

Mercury's magnetosphere exhibits different dynamic regimes. Substorm-like events recorded in the Mariner 10 particle observations (Siscoe et al., 1975) gave rise to problems concerning the inherent nature of these phenomena and prompted the suggestion that the enhancements recorded were generated by solar wind driven fluctuations (Luhmann et al., 1998). Ultra-low frequency (ULF) waves were also observed in Mercury's magnetosphere (Russell, 1989).

The atmosphere of Mercury is very tenuous and the inner edge of the exosphere, the exobase, is the planetary surface itself. During the Mariner 10 flybys, H, He, and O were detected in the atmosphere by the onboard UV spectrometer (Broadfoot et al., 1974). Later, Na, K, and Ca were detected through ground-based observations (Potter and Morgan, 1985, 1986; Bida et al., 2000). Since the atmospheric pressure at the surface is very low ($<10^{-12}$ bar), the mean-free-path is greater than the scale height. Therefore, the Hermean atmosphere is called a "surface-bounded exosphere" (Killen and Ip, 1999).

Sodium, which has a very bright resonant line, Na D, has been hitherto the most investigated among the six species, detected at Mercury. Potter and Morgan (1990, 1997), Potter et al. (1999) and Sprague et al. (1997) found that the exospheric sodium is often concentrated at northern or southern high latitudes and that its distribution varies rapidly. Killen et al. (2001) concluded that sputtering by solar wind particle precipitation in the magnetospheric cusp regions is the source mechanism of sodium at high latitudes. Sprague et al. (1990), on the other hand, suggested that grain boundary diffusion of Na and K from the regolith could provide the abundance of these species in the atmosphere under some conditions. Sprague (1992) described a model where ion impact on the nightside and subsequent diffusion and thermal desorption on the day side could explain the day/night asymmetry in column abundance of these constituents. Five-year Na and K observations were reported to show that a strong and important association of Na and K with radar and visible bright spots on Mercury's surface is present (Sprague et al., 1998). One of the most outstanding coincidences of Na emission associated with radar bright spot at high latitudes is described in Sprague and Massey (2007). However, the images of sodium emission obtained from 1997 to 2003 by Potter et al. (2006) showed no evidence of a topographic effect. Recently, 6-h continuous observations did not show any significant fluctuation in sodium column density when averaged over the visible region (Kameda et al., 2007).

Hunten and Sprague (1997) reported that the average column density of sodium atoms on the dawnside is larger by a factor of 3 than on the dusk side. It was inferred that, on the dawnside, a large fraction of sodium atoms is implanted on the cold surface during the night. On the dusk side, in contrast, most of the sodium atoms implanted on the surface would already have been removed (Leblanc and Johnson, 2003). Schleicher et al. (2004) observed an excess absorption in the solar sodium D2 line during the transit of Mercury across the solar disc and thereby confirmed that the sodium density on the dawnside was higher than on the dusk side. These observations also show two zones of high Na exospheric density near the poles, whit a prevalence of the Northern one. Mura et al. (2008) have compared these observations with the results of a numerical model, which include chemical sputtering as a result of proton precipitation, and the subsequent photon-stimulated desorption (PSD) of Na from the surface. They concluded that concurrent action of chemical sputtering and PSD are able to explain both dawn–dusk and latitudes asymmetries.

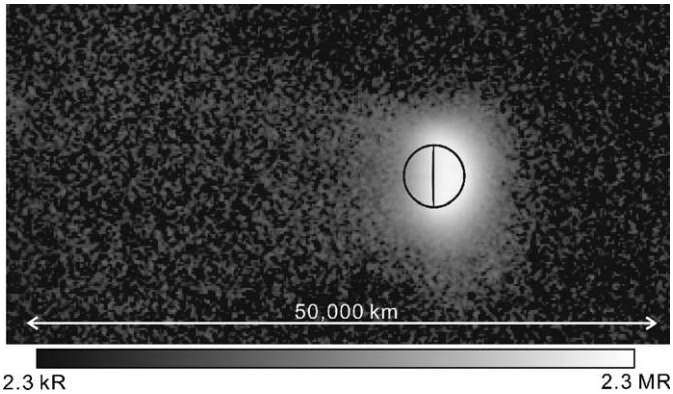

Fig. 1. Na D2 emission line intensity observed using a Fabry–Perot interferometer on 14 June 2006. A faint sodium tail is visible in the anti-Sun direction (the Sun is on the right) (Kameda et al., 2008).

Ip (1986) and Smyth and Marconi (1995) predicted that Mercury's sodium exosphere should be extended in the anti-solar direction because of solar radiation pressure. Conservation of momentum requires that sodium atoms be accelerated in the anti-solar direction, because sodium D line scattering is almost omni-directional. Potter et al. (2002) and Kameda et al. (2008) observed Mercury's sodium tail (Fig. 1) and estimated the lifetime of Na photo-ionisation.

3. Magnetosphere–exosphere–upper surface of Mercury from models

3.1. Magnetosphere

It is believed that the magnetic field in Mercury's magnetosphere is made up of both internal (from the planet) and external contributions. To first order, the intrinsic magnetic field can be represented by a dipolar field with a strength at the equator of about 300–350 nT (Connerney and Ness, 1988; Korth et al., 2008). This leads to a dynamo-related problem concerning the origin of Mercury's magnetic field, which is much weaker than the field strength obtained through scaling down the Earth's magnetic field to the size of Mercury (Glassmeier et al., 2007a, b). The large libration of the planet recently found by radar observations suggests the existence of a liquid core (Margot et al., 2007), which is a necessary condition for a dynamo to operate. Since the weakness of Mercury's magnetic field cannot be explained by simply scaling to the Earth's case, various alternatives have been proposed for describing the Hermean dynamo such as the shell dynamo (Stanley et al., 2004), the deep dynamo (Christensen, 2006), and the feedback dynamo models (Glassmeier et al., 2007a, b).

The external parts of the magnetic field come from currents flowing in the magnetosphere. In the case of Mercury, the magnetopause current and the magnetotail currents provide the most important sources. Since Mercury's magnetosphere is small and the boundary of the magnetosphere (magnetopause) is close to the planet's surface, the field generated by the Chapman–Ferraro current (the magnetopause current) is estimated to be about 50–150 nT on the planetary surface (Glassmeier et al., 2007a, b), which is a substantial fraction of the intrinsic field intensity. The combination of the electrically conducting sub-surface and temporary varying external magnetic field would in addition induce a magnetic field whose magnitude is estimated to be about 5–10% of the internal field (Grosser et al., 2004). The photo-ionisation of exospheric atoms creates an ionised thermal plasma population, especially on the dayside (e.g. Milillo et al., 2005). The ion population is not dense enough to be considered to compose as an ionosphere with the capability to shield the planet from the magnetospheric magnetic and electric fields. Hence, it is referred to as an exo-ionosphere. The ions are energised immediately by electromagnetic fields and become part of the magnetospheric ion population. The lack of an ionosphere causes the current system in the Hermean magnetosphere to be completely different from that at the Earth. Indeed, without an ionosphere, it is not presently clear where and how the magnetospheric current system closes at the planet.

The investigation of how the smaller spatial scale and lack of an ionosphere might affect magnetospheric processes is one of the main objectives of the present missions to Mercury. For example, it is not clear how the processes in the Hermean magnetosphere resemble the processes that take place in other magnetospheres. Important related questions include: (1) How effectively does the magnetosphere store energy in the magnetotail (e.g. Luhmann et al., 1998) and later release it? (e.g. Christon et al., 1987); (2) How effectively does the magnetosphere shield the planet from solar wind particles? (3) How does the direct interaction between the magnetosphere and the planet's surface take place? (4) What is the role of kinetic and electrodynamics effects? These important open questions call for detailed measurements and modelling efforts.

The most frequently used modelling approach is to use a rescaled/modified terrestrial magnetic field model such as: the Luhmann–Friesen model (e.g. Delcourt et al., 2003), Tsyganenko's models (e.g. Luhmann et al., 1998; Massetti et al., 2003; Korth et al., 2004; Scuffham and Balogh, 2006) and the IMF-B_x–interconnected Toffoletto–Hill model (e.g. Massetti et al., 2006, 2007; Sarantos et al., 2001, 2007). The Tsyganenko model (Tsyganenko, 1995) is basically an empirical model constructed by providing a fit to a multitude of observations and by parameterising various solar wind and interplanetary magnetic field (IMF) conditions. Although this model incorporates effects due to the magnetopause current (Chapman–Ferraro current), the tail current (plasma sheet current), the field-aligned currents (region I/II currents), and the ring current, in its application to Mercury, only the magnetopause and the tail current are taken into account. This point is currently controversial and indicates the general difficulty associated with modelling efforts (see the review by Glassmeier, 2000). Another major concern regarding the use of "scaled" Earth models of the magnetosphere is the very different interplanetary conditions pertaining at 0.3 AU as compared with 1 AU. In this regard, Slavin and Holzer (1979) pointed out the relatively high Alfven speeds and corresponding low Alfven Mach numbers, which make the rate and influence of reconnection at the dayside magnetopause far greater at Mercury than at the Earth. This, for instance, results in higher rates of energy input to the magnetosphere; larger magnetic field components normal to the magnetopause; enhanced fluxes of solar wind ions channelling down to the surface and stronger magnetospheric asymmetries in response to the Maxwell stresses exerted by the connection of the IMF to the magnetosphere (Massetti et al., 2006, 2007; Sarantos et al., 2001, 2007). In general, the models suggest that the Hermean magnetosphere is

tightly coupled to the IMF. The strong contribution of the IMF-B_x component causes the field lines to be nearly always open on the sunward side and to display a strong north–south asymmetry. The broad cusp regions thereby resulting would allow the solar wind to directly impact on a large portion of the dayside surface. With a magnetic and electric field model, we may study the motion of solar wind and planetary ions in the Hermean magnetosphere using single particle MonteCarlo simulations (e.g. Delcourt et al., 2003; Mura et al., 2005). Analytical models provide a means to focus on specific aspects of the ion circulation in Mercury's magnetosphere, including finite-gyroradius effects and energy gain due to centrifugal acceleration (e.g. Delcourt et al., 2003). With knowledge of magnetosheath properties derived from Spreiter's gas dynamic approximation (Spreiter et al., 1966) and the kinetic description of particle injection via reconnection (Cowley and Owen, 1989; Cowley, 1995), analytical models can illustrate how solar wind ions enter the Hermean magnetosphere (Fig. 2) (e.g. Massetti et al., 2006, 2007; Sarantos et al., 2007).

Self-consistent approaches are provided by magneto-hydro-dynamic (MHD) (Gombosi et al., 2000; Kabin et al., 2000; Ip and Kopp, 2002) and hybrid (Kallio and Janhunen, 2003a, 2004; Trăvniček et al., 2007) simulations. MHD models show not only that the Hermean magnetic field can be strongly connected to the IMF, but also that the bow shock and the magnetopause can be very close to the surface during episodes of high solar wind dynamic pressure (Kabin et al., 2000; Kallio and Janhunen, 2003b). A matter of considerable concern regarding MHD models is the large ion gyroradius with respect to the geometrical dimensions of Mercury's magnetosphere. While the overall picture provided by MHD results stay the same, hybrid modelling including ion kinetic effects can pinpoint the locations where protons (Kallio and Janhunen, 2003b) and multiply charged heavy ions (Kallio et al., 2008) from the solar wind impact the planet's surface. In particular, this hybrid model shows that the solar wind protons form two high ion-impact flux regions on the Hermean surface: "auroral" region and cusp region. The former region is located around the magnetic poles near the open-closed field line boundary while the latter region is sited near the magnetic cusp. Occasionally, when the solar wind dynamic pressure is high, the proton-impact flux can be substantially enhanced over the whole dayside hemisphere compared with the nominal upstream situation. The multiply charged heavy solar wind ions also impact predominantly near the magnetic cusps but the "auroral" impact region is not so pronounced as it is in the impacting protons case. The dawn–dusk ion-impact flux asymmetry also increases when the mass per charge ratio (m/q) of the impacting ion increases. Fig. 3 provides an overview of Mercury's magnetosphere obtained using this hybrid model.

Field-aligned currents (FAC), identified as "Region 1" currents in the Earth's magnetosphere, are the dominant means by which momentum and energy are transferred from magnetospheres to the planet (Kivelson, 2005). Mercury will have field-aligned currents that have been observed by Mariner 10 (Slavin et al., 1997), but the understanding regarding the properties of FACs when there is no conducting ionosphere and the implications of this unique set of low altitude boundary conditions for the electrodynamics of Mercury's magnetosphere are yet unclear (Slavin, 2004). The current closure at the surface is one possible explanation of the observations. Hill et al. (1976) estimated the regolith electrical conductivity of about 0.1 mho. The conductivity of the planetary surface was also investigated using a hybrid model to investigate

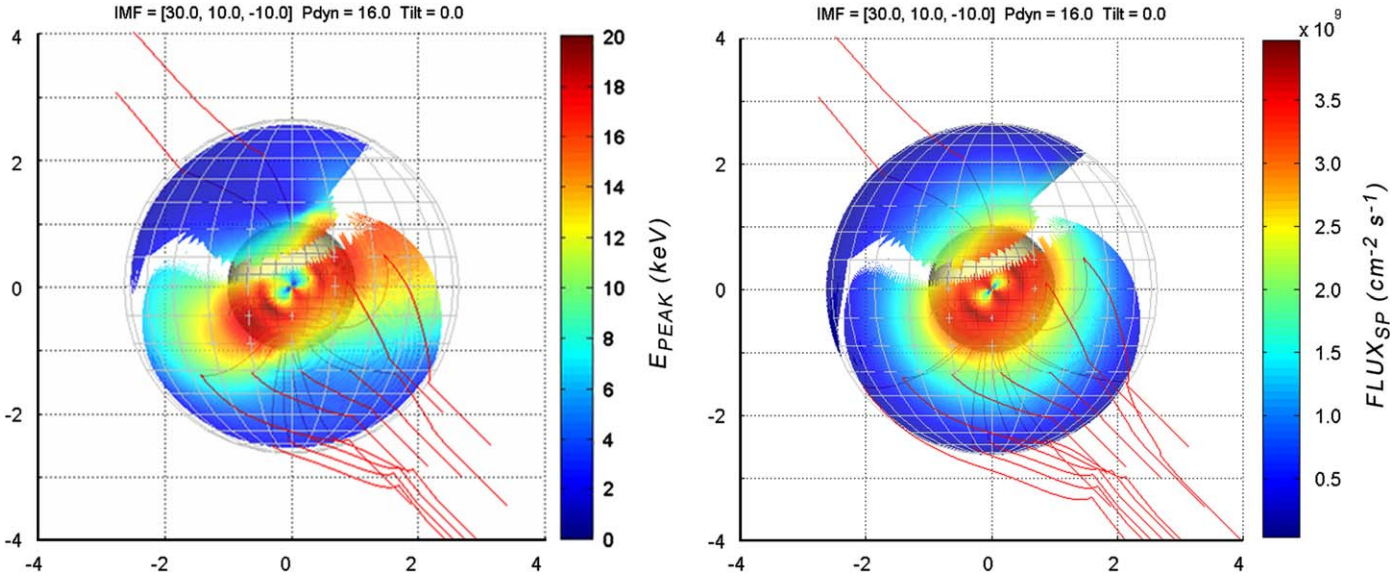

Fig. 2. Left: peak energy of protons injected across the open dayside magnetopause. Right: proton flux on the inner side of the magnetopause. The parameters have been calculated by assuming IMF: 30, 10, and −10 nT, $V_{SW} = 400$ km/s and $D_{SW} = 60\,cm^{-3}$ (Massetti et al., 2007).

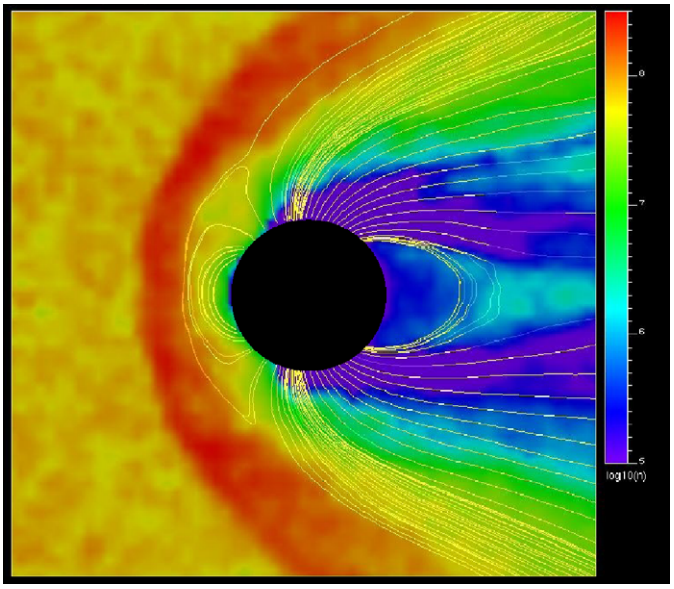

Fig. 3. Hermean magnetosphere based on a hybrid model. The colour shows the density of the solar wind protons in $\log 10\,m^{-3}$ from 5 to 8.5. The yellow lines represent the magnetic field (Kallio et al., 2008).

how a current system closes in the magnetosphere (Janhunen and Kallio, 2004).

Various ULF wave generation mechanisms are known to operate in the Earth's magnetosphere (e.g. transmission of solar wind fluctuations into the magnetosphere, Kelvin–Helmholtz vortices generated at the magnetopause and instabilities due to kinetic effects). While ULF waves in the Earth's magnetosphere are conveniently described using MHD, at Mercury the ULF waves have been observed (Boardsen et al., 2008), but a different approach is needed to simulate them because none of these waves are likely to be of sufficiently low frequency to allow ion kinetic effects to be ignored (Blomberg, et al., 2007; Glassmeier and Espley, 2006; Glassmeier et al., 2003, 2004).

Unthermalised heavy ions do not move with the protons and with the rest of the magnetospheric plasma. Rather, they simply execute single particle motion that, due to their large gyro-radii, causes them to be very quickly lost to the surface or solar wind. In order for these heavy planetary ions to be assimilated into the magnetospheric plasma populations, the ring and shell distributions they create must be relaxed through wave–particle interactions that act to scatter the planetary ions. However, Boardsen and Slavin (2007) found no evidence in the Mariner 10 data of these expected ion cyclotron waves. Further, their results suggested that wave modes cannot grow within such a small magnetosphere. In the absence of wave–particle interactions, heavy planetary ions will not be incorporating into the magnetospheric plasma populations or reside therein for sufficient time to influence magnetospheric substorms and dynamics.

Energetic electrons are known to be present in the magnetospheres of the Earth, Jupiter, and Saturn and they assume increasingly more aligned pitch angle distributions when approaching these planets. The temperature anisotropy present in the inner-magnetospheres of these bodies can excite whistler-mode chorus emission (Katoh and Omura, 2007) that is believed to be the local agent of electron acceleration to relativistic energies. The ratio of the electron plasma frequency to the electron cyclotron frequency is the parameter that determines the energy range of resonant electrons. If the plasma density is relatively high so that this ratio attains a value of ~5, the acceleration of resonant electrons is very efficient. If the energy of the injected electrons becomes of the order of several hundred keV, relativistic turning acceleration (RTA) (Omura et al., 2007) sets-in and subsequently ultra-relativistic acceleration (URA) may result (Summers and Omura, 2007). This can take place in less than 1 s and does not necessarily require a large volume. Since Mercury is lacking in quasi-trapped electrons and the loss cones of these particles are huge due to the relatively small difference between the magnetic field strength in the equatorial plane of the magnetosphere and the point where the magnetospheric flux tubes intersect the surface of the planet, if intense fluxes of relativistic electrons are detected in the small magnetosphere of Mercury this will be a pleasant surprise.

3.2. Exosphere

Atoms and molecules may be ejected from Mercury's surface by several mechanisms with various temporal and spatial distributions, with different energy signatures and with variable composition with respect to surface composition (see Section 4.4). Several studies (Hunten et al., 1988; Killen and Ip, 1999; Killen et al., 2001, 2007; Wurz and Lammer, 2003; Milillo et al., 2005; Leblanc et al., 2007) have already described such mechanisms in detail; hence, we will here only summarise present knowledge regarding surface release processes. At the present time, five mechanisms are usually cited as potentially important to the formation of Mercury's exosphere:

- Thermal desorption (TD) or evaporation was suggested to explain the Hydrogen profiles observed by Mariner 10 around Mercury (Hunten et al., 1988), and this explanation was later generalised to all volatile species (Hunten and Sprague, 2002). The energies of released particles are low so that associated particles generally re-impact the surface (see Fig. 4, panel a).
- PSD was invoked as an explanation after the first observation of sodium emission from the Mercury's exosphere (Potter and Morgan, 1985; McGrath et al., 1986). The particles thereby released are volatiles and their energy distribution produces a higher altitude profile. Thus, a fraction of PSD-released particles escapes from the planet (see Fig. 4, panel b).
- Solar wind sputtering and, more generally, charged particle sputtering, has probably been the most

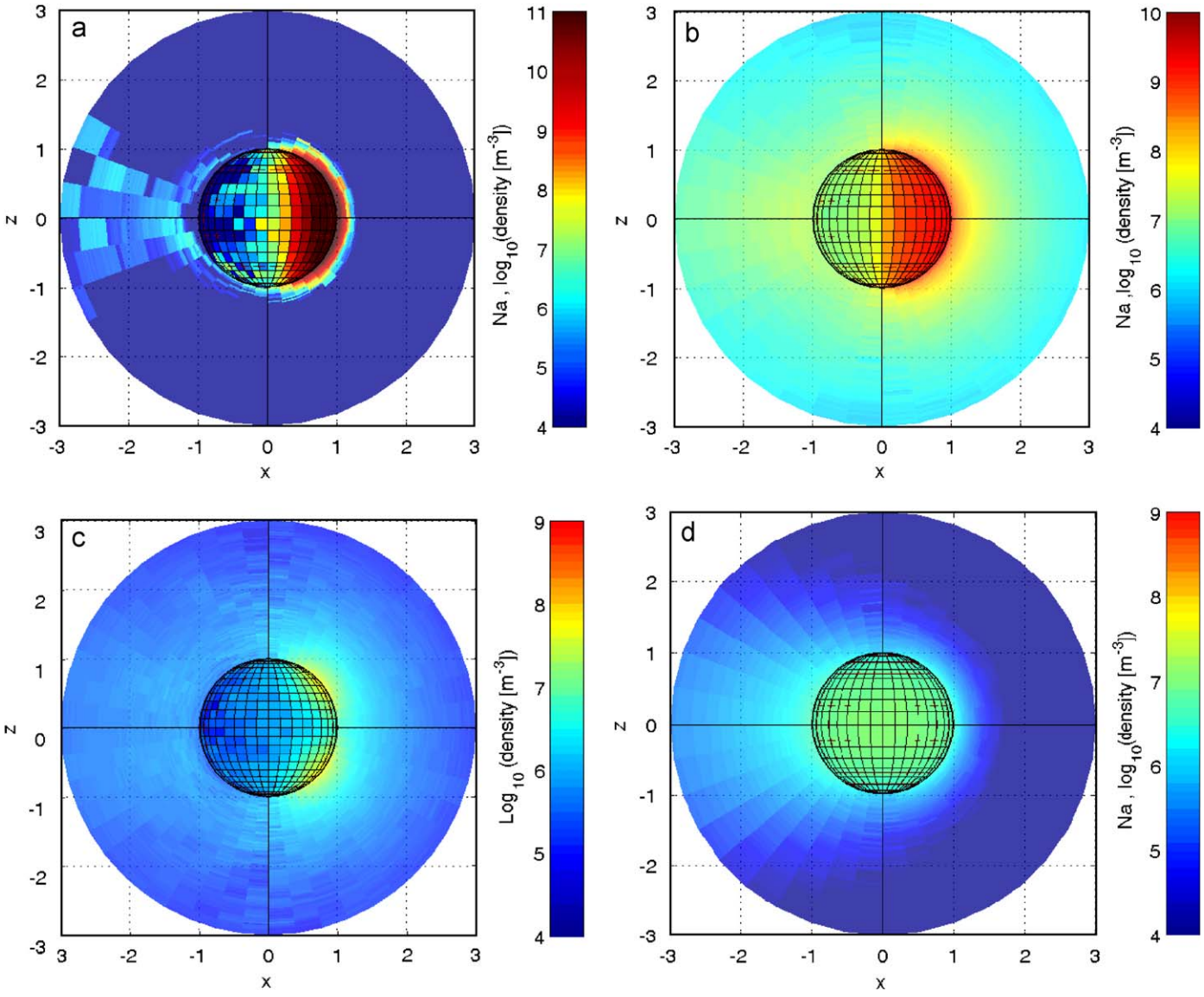

Fig. 4. Exospheres modelled for different surface release processes: (a) TD, (b) PSD, (c) ion-sputtering, and (d) MIV (from Mura et al., 2007).

discussed mechanism since observational evidence of bright spots at high latitude and their short time variations with respect to Mercury's day were reported (Potter and Morgan, 1990). This process depends on plasma precipitation and is therefore highly localised and variable (Kabin et al., 2000; Kallio and Janhunen, 2003b; Massetti et al., 2003; Mura et al., 2005). A recent numerical study by Delcourt and Seki (2006) indicated that the precipitation pattern of Na^+ largely depends on magnetospheric convection. It was also suggested that the concerned convection pattern is controlled not only by the solar wind but also by surface conductivity. Furthermore, the released species are not only volatiles, but also refractories (e.g. Ca, Mg, etc.; Wurz et al., 2007). Since the process has a wide energy spectrum of up to more than ~100 eV depending on the released species (Sigmund, 1969; Sieveka and Johnson, 1984), the altitude profile related to this process has a higher scale height than that pertaining to other release processes (Mura et al., 2007) (see Fig. 4, panel c).

- Meteoroid impact vaporisation (MIV) was identified very early as a potentially important mechanism (Morgan et al., 1988) for the production of Mercury's exosphere and it is now considered to be a key mechanism in maintaining a global balance between the sinks and sources of Mercury's exosphere (Cremonese et al., 2005, 2006). Up to now, the population of dust at Mercury has been extrapolated from calculations performed for the Earth (Zook, 1975) based on quite old models (Erickson, 1968; Southworth and Sekanina, 1973). All the soil in the impacted volume may, depending on the projectile's size and velocity, be vaporised. The energy distribution peaks at a few eV (see Fig. 4, panel d).

- Chemical sputtering has also been cited as potentially leading to a substantial ejection rate from Mercury's surface (Potter, 1995; Mura et al., 2008). It may also have a strong effect on the surface structure through radiolysis and photolysis (Johnson and Quickenden, 1997).

The most debated questions regarding these different processes are as follows:

- What are the relative densities of the generated exosphere? What are the relative efficiencies of these processes?
- What are the energy distributions of those atoms ejected from the surface? What and where are the sources and sinks of the exosphere?
- What are the differences between the spatial distributions of active processes at the surface?
- How do their temporal variations vary during annual or diurnal cycles?

Beyond the characterisation of the ejection mechanisms, the following key issues need, in addition, to be addressed are as follows:

- What is the flux of micrometeoroids at Mercury's heliocentric distance?
- Is there a depletion of elements at the dayside surface that leads to a competition between different mechanisms?
- What is the role of surface diffusion through the pores of the regolith and through the upper surface grains?
- Does the surface topography play a role in the formation of Mercury's exosphere as suggested by Sprague et al. (1990). If so, what kind of exospheric signatures can be expected?
- What is the role of Mercury's magnetosphere, magnetospheric ion sputtering and recycling in the formation of Mercury's exosphere?
- What characterises the day to nightside circulation and what is the role of solar radiation pressure?

4. Measurements and goals of the BC mission

4.1. Hermean environment viewed by the BC mission

The inter-instrument collaborations planned onboard each spacecraft of the BC mission and the opportunities afforded to perform two-point simultaneous measurements at Mercury constitute exciting features of the mission.

A 1:4 resonant orbit configuration for the two spacecraft is currently considered so that the closest approach between the two satellites will be a few 1000 km. Before that during the first 2 weeks in orbit, the two spacecraft will have a few close encounters (few tens of kilometres of each other when close to periherm). Fig. 5 shows an example of four consecutive MPO orbits and one MMO orbit around Mercury for the closest mutual approach that is sketched in panel c. The local times of the orbital planes are not presently known for the time being, so it is not yet possible to define the meridional plane of the orbits. Thus, MMO apoherm could be in the solar wind, in the magnetotail, or somewhere in the dawn–dusk plane (Fig. 6). However, one can see that for one MMO orbit there will be opportunities for different kinds of coordinated observations. It should be kept in mind that as the gravity field of Mercury is not well known before the MESSENGER observations and in addition the large solar radiation pressure can cause unpredicted changes in the orbits of the satellite, one cannot be completely confident now regarding orbital evolution. However, irrespective of these details, the peculiar configuration during closest approach will permit inter-calibration measurements to be made between similar instruments on MMO and MPO and support small-scale temporal and spatial studies of specific phenomena.

The question as to whether the exosphere varies substantially when large solar wind disturbances arrive is a very interesting issue, which can best be addressed by making multi-point observations through coordinated MPO-MMO operations. MMO can monitor the solar wind, while MPO observes, at low-altitudes, changes in the exosphere in response to changing solar wind conditions. In extreme cases, the solar wind dynamic pressure can be so much elevated that it is not possible for the magnetic field to continue to stand-off the solar wind pressure. Under these circumstances, the whole dayside surface may be directly exposed to the solar wind. How the enhanced sputtering process will then change the exosphere is an intriguing question.

Similarly, investigations as to how variations in the exosphere affect magnetospheric dynamics are best studied by coordinating MPO–MMO measurements when MMO is in the magnetosphere. A very interesting question in this context is whether the exospheric plasma source can so heavily load the magnetosphere that a unique dynamical behaviour will emerge due to the presence of multi-ion species (the heavy mass density may be even greater than the solar wind density). These are situations that do not occur in the Earth's magnetosphere and we thus do not have direct knowledge concerning them.

The propagation of magnetospheric effects down to low altitudes is an equally important issue. This gives rise to aurorae at Earth; the puzzle here is that at Mercury there is no ionosphere, which is a crucial element in the theory of auroral stimulation. Nevertheless, particle precipitation will occur in an auroral zone and may thus result in uniquely different Hermean auroral phenomena.

4.2. BC instruments to study the environment

The instruments devoted to Hermean environment investigations during the BC mission are briefly described below. In Table 1, a summary of the scientific objectives ranging from the magnetosphere to the surface and major

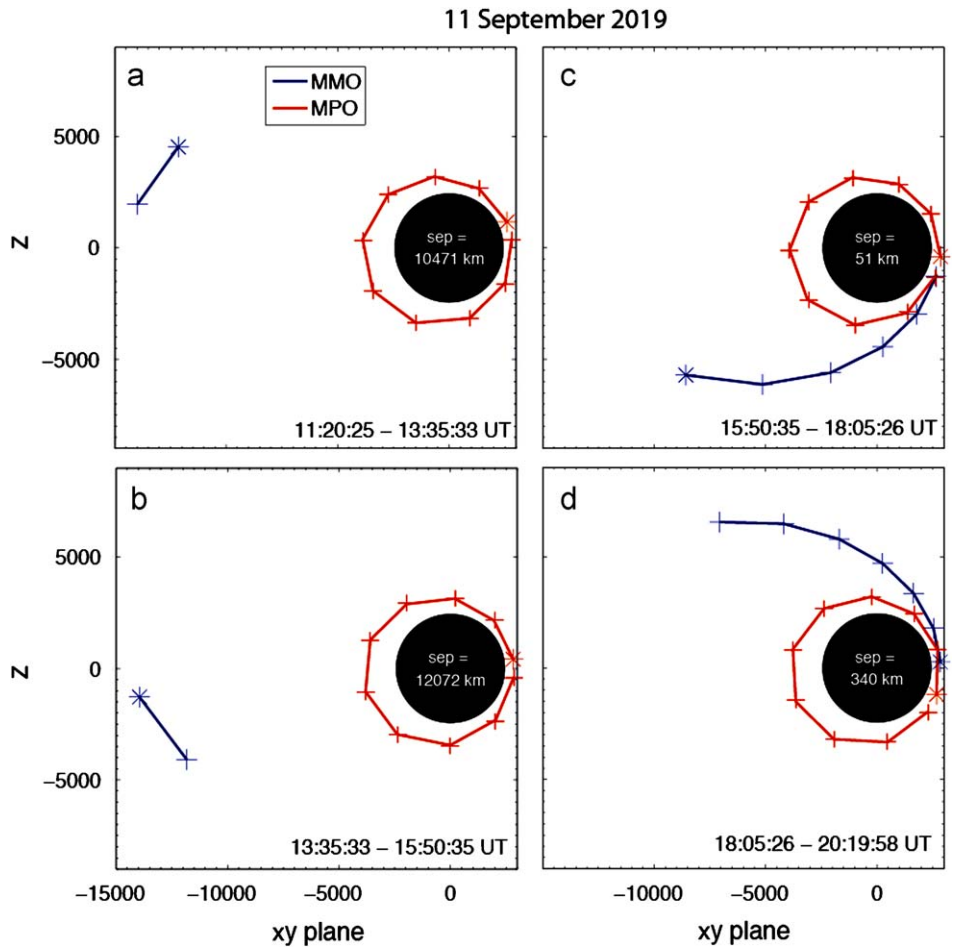

Fig. 5. Four consecutive MPO orbits (red lines) are executed while MMO makes one orbit (blue lines) around Mercury. Sharp changes seen in the orbits are caused by the low-resolution of the orbit file; star signs show the start of the trajectory and + signs give the actual positions of the orbit files. The black circle represents Mercury and the minimum separation between MPO and MMO for a given MPO orbit is shown in the middle of each circle.

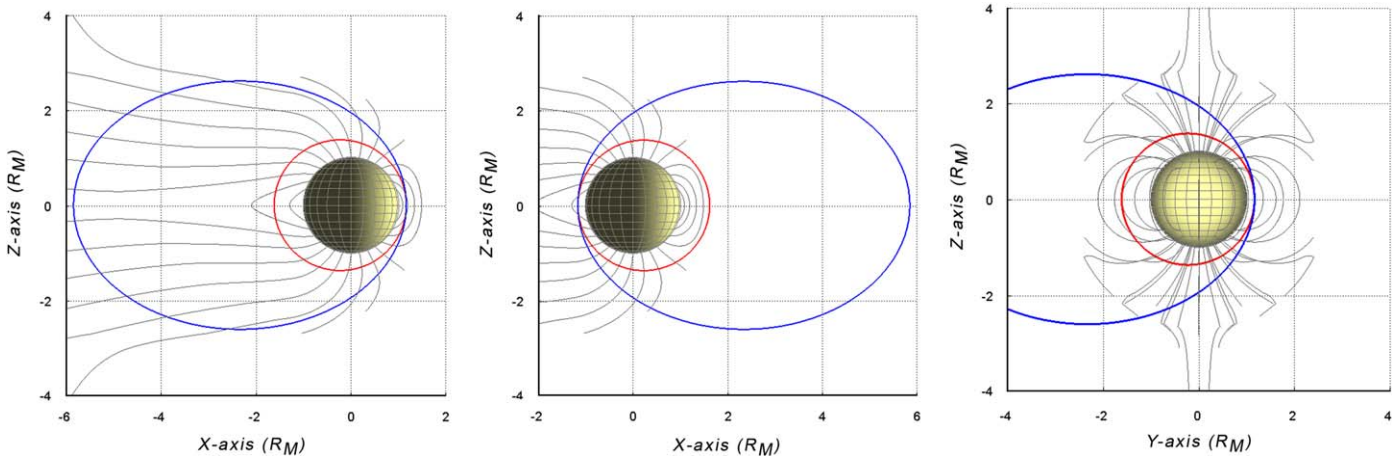

Fig. 6. Sketch of MPO and MMO orbit configurations (red and blue, respectively) during the BC mission with respect to Hermean magnetosphere. Both orbits will have apoherm in the magnetospheric tail when Mercury is close to apohelion (left panel). Both orbits will have apoherm in the dayside (out of the magnetosphere) when Mercury will be close to perihelion (centre panel). Other configurations will include both orbits in dawn-dusk orbits (right panel).

scientific goals (related to the environment only) of the instruments on the BC mission are presented.

MERMAG (consortium of MPO/MAG and MMO/MGF) (Baumjohann et al., 2008; Glassmeier et al., 2008) are dual, tri-axial fluxgate magnetometers which are able to distinguish between natural signals and the magnetic influence of the spacecraft. The primary objective of MPO/MAG is to provide accurate measurements of the

Table 1
BepiColombo instruments for Hermean environment.

Responsibility	Instrument		Target	Scientific objective for environment
PI: K.-H. Glassmeier (Germany) Co-PI: C. M. Carr (UK)	MERMAG	MPO/MAG	Vector magnetic field (accuracy 10 pT and time resolution up to 128 Hz)	Planetary field
PI: W. Baumjohann (Austria) Co-PI: A. Matsuoka (Japan)		MMO/MGF		Formation and dynamics of magnetosphere
PI: Y. Kasaba (Japan) Co-Pis: J.-L. Bougeret, L. Blomberg, H. Kojima, S. Yagitani Lead-Co-Is: M. Moncuquet, J. G. Trotignon, G. Chanteur, Y. Kumamoto, Y. Kasahara, Y. Omura	MMO/PWI	EWO(OFA/WFC/EFD) SORBET AM^{2}P WPT MEFISTO LF-SC DB-SC	DC electric field, plasma waves, radio waves: • Electric field (DC ~10 MHz) • Magnetic field (0.1 Hz–640 kHz) • Electron density and temperature	Structure of the magnetosphere, dynamics of the magnetosphere, energy transfer and scale coupling wave–particle interactions, solar radio emissions and diagnostics (including boundaries of different regions of the magnetosphere, kinetic processes associated with the dynamic variation of the magnetosphere, shocks and discontinuities of the magnetosphere)
PI: Y. Saito (Japan) Co-PIs: J.-A. Sauvaud (France), M. Hirahara (Japan), S. Barabash (Sweden) Lead-Co-Is: D. Delcourt (France), K. Asamura (Japan), T. Takashima (Japan)	MMO/MPPE	MEA, HEP-ele, MIA, MSA, HEP-ion, and ENA	Electrons (3 eV–30 keV, 30–700 keV), ions (5 eV/q–30 keV/q, 5 eV/q–40 keV/q, 30 keV–1.5 MeV), and energetic neutral atoms (<25 eV–3.3 keV)	1. Structure, dynamics, and physical processes in the Mercury magnetosphere 2. Interaction between surface, exosphere, and magnetosphere 3. Collisionless shock physics in the inner heliosphere
PI: S. Orsini (Italy) Co-PIs: S. Livi (USA), S. Barabash (Sweden), K. Torkar (Austria)	MPO/SERENA	ELENA	ENA (20–5000 eV) ($4.5^\circ \times 2.4^\circ$ angle resolution, 10% velocity resolution)	Neutral gas escaping from the planet and the related processes
		STROFIO	Neutral atoms (60 M/DM mass resolution)	Dayside and nightside exosphere composition and structure. Exospheric sources and sinks
		MIPA	Ions (10 eV–15 keV) (energy and angle resolution rough mass resolution)	Plasma precipitation toward the surface and ions circulation
		PICAM	Ions (10 eV–3 keV) (variable energy and angle resolution, 100 M/DM mass resolution)	Exo-ionosphere extension and composition, and the close-to-planet magnetospheric dynamics
PI: E. Quemerais (France) Co-PIs: S. Okano (Japan), O. Korablev (Russia)	MPO/PHEBUS		Exospheric emission between 55 nm and 315 nm (spectral resolution between 1 and 1.5 nm)	Exospheric composition, 3D structure and dynamic characterization of the exospheric sources and sinks
PI: I. Yoshikawa (Japan)	MMO/MSASI		Dayside Na emission (spectral resolution ($\lambda/\partial\lambda$) is ~90,000, field of view 30°)	Na density profile, north–south asymmetry, dawn–dusk asymmetry, and sodium tail extended to the antisolar direction
PI: K. Nogami (Japan)	MMO/MDM		Dust impact momentum, speed, direction, and the number of impacts	Detect interstellar dust (>1 μm), cometary dust, beta meteoroids, dust from Mercury and dust to Mercury, which might contribute to the formation of tenuous atmosphere
PI: J. Huovelin (Finland) Co-PI: M. Grande (UK)	MPO/SIXS		X-ray (spectral range: ~1–20 keV; including X-ray flare parameters), protons (spectral range: ~1–30 MeV) and electrons (spectral range: ~100 keV–3 MeV)	X-rays and energetic particles in the Hermean environment

Table 1 (*continued*)

Responsibility	Instrument		Target	Scientific objective for environment
PI: G. Fraser (UK)	MPO/MIXS	MIXS-C	X-ray fluorescence (0.5–7.5 keV range)	Elemental (Si, Ti, Al, Fe, Mg, Ca, O, Na, K, Ni, Cr, P) surface composition, global mapping and composition of surface features.
Co-PI: K. Muinonen (Finland)		MIXS-T		Auroral emission
PI: E. Flamini (Italy)	MPO/SIMBIO-SYS	STC	Stereo global mapping (50 m spatial resolution at 400 km altitude)	Topography can be useful to understand the surface–exosphere relation. Identify the source
Co-PIs: F. Capaccioni (Italy), L. Colangeli (Italy), G. Cremonese (Italy), A. Doressoundiram (France), Y. Langevin (France), J.L. Josset (Switzerland)		HIRC	High spatial resolution mapping of selected areas (5 m spatial resolution at 400 km altitude)	minerals for each of the constituents of Mercury's exosphere and the identification of the mineralogical composition of potential "bright spots"
		VIHI	Global mineralogical mapping (spectral resolution 0.4–2.2 μm; <500 m spatial resolution) and compositional characterization of selected areas (100 m spatial resolution)	
PI: H. Hiesinger (Germany)	MPO/MERTIS		Global mineralogical mapping: spectrometer channel (spectral range 7–14 μm, spectral resolution <200 nm) radiometer channel (spectral range up to 40 μm)	Identify the source minerals (feldspars, silicates, Fe-free pyroxenes and Fe-free olivines and the plagioclase) for each of the constituents of Mercury's exosphere. Thermo-physical properties of the surface like thermal inertia and internal heat flux
Co-PI: J. Helbert (Germany)				

Mercury's intrinsic magnetic field. The primary objective of MMO/MGF is to study the formation and dynamics of Mercury's magnetosphere and the processes that control the interaction of the magnetosphere with the solar wind and with the planet itself. The combination of both magnetometers provides a unique opportunity to study cause and effect relationships, as well as the propagation of waves in the magnetosphere and substorm disturbances.

MMO/PWI (Plasma-Wave Investigation) is a system of several instruments designed for plasma wave investigations (Kasaba et al., 2008). It measures plasma waves, electromagnetic waves from DC to 10 MHz, DC electric fields, electron density and temperature in and around the Hermean magnetosphere. The dynamic spectra of electrostatic and electromagnetic waves, covering the proton and electron cyclotron frequencies, will be obtained within the magnetosphere with 4 s time resolution. Coupled with the boundaries of different regions of the magnetosphere, a variety of plasma waves are expected to be observed, providing a unique opportunity for clarifying the kinetic processes associated with dynamic variations in the magnetosphere. Some segments of the waveforms sampled at 360 kHz will be recorded for the identification of nonlinear waves; ion holes and electron holes carried by non-thermal particle components and generated at shocks and discontinuities in the magnetosphere. Wave number vectors of electromagnetic waves at several spectral peaks at higher frequencies (<10 MHz) will also be measured to detect solar radio bursts, possibly in collaboration with an experiment aboard Solar Orbiter.

MMO/MPPE (Mercury plasma particle experiment) (Saito et al., 2008) will observe the electrons (3 eV–700 keV), ions (5 eV–1.5 MeV), and energetic neutral atoms (25 eV–3.3 keV) using six sensors (MEA, HEP-ele, MIA, MSA, HEP-ion, and ENA). The scientific objectives of MPPE are categorised into three core groups: (1) structure, dynamics, and physical processes in Mercury's magnetosphere, (2) interactions between the surface, exosphere, and magnetosphere, and (3) collisionless shock physics in the inner heliosphere. The formation and characteristics of the small temporal- and spatial-scale Hermean magnetosphere will be investigated using high time-resolution plasma observations. To investigate the plasma supply from the solar wind as well as the ion composition of the exosphere, MSA, HEP-I and ENA measurements are required. In order to study the stability of the plasma sheet of Mercury's small magnetosphere, high time-resolution electron observations made by MPPE/MEA and HEP-e, together with wave observations obtained at around the LHD frequency by PWI are important. With regard to substorms at Mercury, recent simulation studies showed that the non-adiabatic acceleration of electrons as well as of ions during dipolarisation events (Delcourt et al., 2005, 2007) can be present. Thus, both the ion and electron sensors (MEA, HEP-ele, MIA, MSA, HEP-ion) will provide important information concerning: the frequency of occurrence and the time-scale

of substorms; carriers of FAC and the effects of the presence of heavy ions. Observations of the phase space density by MPPE will also be important in order to examine particle acceleration, trapping, and loss in the Hermean magnetosphere, especially during energetic electron bursts, such as those recorded aboard Mariner 10 (e.g. Christon et al., 1987). Ion and ENA composition measurements by MPPE/ MSA, HEP-ion, and ENA observations are essential in order to understand interactions between Mercury's surface, exosphere, and magnetosphere. Since it is presently suspected that the convection pattern is controlled not only by the solar wind but also by surface conductivity, precise observations of plasma flow (by MEA and MIA) will provide important information concerning the magnetosphere–surface interaction.

MPO/SERENA (Search for Exospheric Refilling and Emitted Natural Abundances) (Orsini et al., 2008b) will observe the thermal and energetic neutral atoms and ion particle populations in the near-planet environment. This instrument suite comprises two neutral particle analysers (ELENA and STROFIO) and two ion spectrometers (PICAM and MIPA). ELENA will observe neutrals at energies above 20 eV thereby, determining the velocity and spatial distribution of neutral gas escaping from Mercury, it will investigate the processes responsible for this escape. STROFIO will observe the composition of the exospheric gas thermal component. PICAM will observe ions in the energy range 10 eV–3 keV with good mass resolution and wide FoV; its primary goals are to determine the extension and composition of the exo-ionosphere and to investigate magnetospheric dynamics close to the planet. MIPA will detect ions in the energy range 10 eV–15 keV and will, thus, monitor plasma precipitation toward the surface as well as those ions that are energised and transported throughout the environment of Mercury.

MPO/PHEBUS (Probing the Hermean Exosphere By Ultraviolet Spectroscopy) (Chassefière et al., 2008) will monitor Mercury's exospheric optical emissions. PHEBUS is a dual EUV and UV spectrometer with a moving baffle and has been optimised to achieve a sensitivity that is typically 0.1 counts per second per Rayleigh when at its optimum spectral resolution. PHEBUS should be able to scan the exosphere from the surface up ~1500 km altitude when in twilight mode to track heavy and minor species expected to be present in Mercury's exosphere and to scan the altitude emission profile on the dayside from 200 km above the surface (the bright surface of the planet is a limiting factor here). PHEBUS will also characterise the annual and diurnal cycles of Mercury's exosphere having a complete exospheric map eight times a year.

MMO/MSASI (Mercury's sodium atmosphere spectral imager) (Yoshikawa et al., 2008) is a Fabry–Perot interferometer equipped for spectroscopic imaging of the sodium D2 emissions from Mercury's exosphere, thereby enabling the observation of sodium emissions from the dayside. The time resolution of 1 min is far more sufficient to investigate correlations between the solar wind flux observed by the charged particle sensors and the variation in the dayside distribution of sodium density. The 30° field of view will enable the observation of north–south asymmetry, dawn–dusk asymmetry, and the illuminated sodium tail that extends in the anti-solar direction, in fact, since the MMO is a spin-stabilised satellite, field of view of MSASI in the tail direction is several Mercury radii.

MMO/MDM (Mercury dust monitor) will use a piezoelectric zirconate titanate (PZT) sensor (MDM-S) attached to the outside of the side panel of MMO to detect the momentum, speed, direction of dust grains as well as the number of impacts. No measurements of interplanetary dust particles have yet been acquired near Mercury (0.3–0.47 AU). The scientific objectives of the experiment comprise: the characterisation of interstellar dust (>1 μm); cometary dust; beta meteoroids (which move anti-sunward near the Sun with high velocity due to high solar radiation pressure) and dust travelling from and toward Mercury (which contributes to the formation of its tenuous atmosphere).

MPO/SIXS (Solar Intensity X-ray and particle Spectrometer) will monitor X-rays and energetic particles. The primary scientific task is to monitor solar X-ray, energetic proton and electron irradiation in the Hermean environment (Huovelin et al., 2005). A secondary and independent goal concerns the collection of data relevant to studies related to the temporal and spectral variability of the solar X-ray corona, and the properties of energetic protons and electrons near Mercury (Vainio, 2005).

MPO/MIXS (Mercury Imaging X-ray Spectrometer) (Carpenter et al., 2008) will support X-ray fluorescence analysis of the Hermean surface. Its primary science goals include the making of global elemental maps of key rock-forming elements in the main terrain units and high spatial resolution mapping of certain elemental abundances where possible. A secondary goal of the MIXS instrument will be to investigate auroral zone dynamics. In the precipitation regions of energised particles on the surface of Mercury (for example in the vicinity of the magnetospheric cusps on the dayside and/or in regions of substorm induced particle precipitation on the nightside), it is likely that associated X-rays will be produced at the surface. The two downward looking instruments MIXS-C (using a Collimator) and MIXS-T (using a Telescope) will not only be able to study the surface composition (the primary science goal) but may also provide an important link to ongoing remote measurements of the magnetospheric field and plasma environment by MMO.

MPO/SIMBIO-SYS (Spectrometers and Imagers for MPO BC Integrated Observatory SYStem) (Flamini et al., 2008) is an instrument that features three optical channels. The stereo imaging channel (STC) will provide global stereo mapping with a maximum spatial resolution on the surface of 50 m at 400 km altitude. The high-resolution imaging channel (HRIC) will provide high spatial resolution of selected areas at a 5 m pixel scale at 400 km altitude. The Visual and infra-red hyper-spectral

imager (VIHI) will provide global mineralogical mapping at a spatial resolution better than 500 m as well as compositional characterisation of selected areas at a maximum spatial resolution of 100 m. Such knowledge of the surface composition is mandatory to unambiguously identify the source minerals of each of the constituents of Mercury's exosphere and to determine the mineralogical composition of potential "bright spots" (source areas on the surface where Na and K are either stored locally in cold regions or are intrinsically higher in abundance in the surface mineralogy). Also, the gaining of topographic knowledge can be useful when trying to understand surface–exosphere interactions.

MPO/MERTIS (MErcury Radiometer and Thermal infra-red Imaging Spectrometer) is an imaging spectrometer with an integrated radiometer (Hiesinger et al., 2008). MERTIS will globally map the planet with a spatial resolution of 500 m and an S/N ratio of at least 100 (it will exceed 200 for a typical dayside observation). MERTIS will map 5–10% of the surface with a spatial resolution higher than 500 m. In addition, by integration of μ-radiometer data, MERTIS will be able to measure thermo-physical properties of the surface, such as thermal inertia and internal heat flux, and derive from this further information concerning surface texture and structure. The spectral coverage of MERTIS affords the capability to detect feldspars (Helbert et al., 2007). Therefore, FeO- and TiO_2-free silicates (e.g. feldspars, Fe-free pyroxenes and Fe-free olivines) and the plagioclase series ranging from sodium-rich end-member albite ($NaAlSi_3O_8$) to calcium end-member anorthite ($CaAl_2Si_2O_8$) can be detected.

4.3. Magnetosphere from two vantage points

4.3.1. Substorms, FAC and tail-dynamics

Substorms, whose possible signatures were detected by Mariner 10 (see Section 2), are likely to be an impulsive process that lasts for only a few minutes in Mercury's magnetosphere. For this reason, it is crucial to be able to discriminate temporal and spatial variations in the measurements. Substorm signatures are expected to involve different regions and different scales. Signatures of reconnection, dipolarisation, and field-aligned current formation would be present in the magnetotail current sheet. Recent simulation studies showed non-adiabatic acceleration of electrons as well as ions during dipolarisation events (Delcourt et al., 2005, 2007). While these are predicted to be present on the basis of experience at Earth, there are several open questions concerning substorms at Mercury, including whether they can really be considered an analogue of terrestrial substorm processes. For example, it is not clear how: field-aligned currents close in the absence of an ionosphere; how low Alfven Mach numbers at 0.3 AU influence the reconnection process and, finally, how the rate, intensity and time scales of magnetospheric dynamics at Mercury differ from the terrestrial case. Therefore, it is essential to achieve simultaneous two-point measurements at Mercury so as to capture the cross-region coupling aspects of substorm processes.

If the two spacecraft are each located in the night-side magnetosphere (Fig. 6, left panel), it will be possible to catch a substorm event using different observational methods. First the magnetic field measurements of MMO/MGF and MPO/MAG will register signatures of stretching and dipolarisation of the magnetic field lines as well as disturbances related to magnetotail reconnection plasmoids, and field-aligned currents. Also, the ion and electron sensors of MMO/MPPE will provide important information about the time scale of substorms, carriers of field-aligned currents and the effects of heavy ions. Plasma injections will be monitored at two points, MMO/MPPE and MPO/SERENA, during its evolution. Observations of phase space density are important in investigating particle acceleration, trapping, and losses in Mercury's magnetosphere, especially during energetic electron bursts which were observed by Mariner 10 (e.g. Christon et al., 1987). Furthermore, two spacecraft measurements of the magnetic field may allow us to determine the wave modes that are produced in the course of a substorm.

Although limited in time, there will be occasions when MMO is outside the magnetosphere while MPO is in the inner tail (Fig. 6, centre panel). This configuration can support studies of responses in the magnetotail to sudden solar wind and IMF changes. This kind of investigation may be more important at Mercury than at Earth since whether tail dynamics are driven directly by the solar wind or not is yet to be established in the mysterious planet case.

4.3.2. Dayside and nightside reconnection

In the Earth's magnetosphere, magnetic reconnection is considered to be the key driving process for the transfer of mass, momentum and energy as well as for the energisation of magnetospheric plasma particles. Since Mercury's magnetosphere has essentially the same configuration as that of Earth and since its magnetic dipole moment has a similar orientation, it is natural to anticipate that reconnection phenomena at Mercury will constitute an important process. The challenge to this lies in the smallness of the magnetosphere. Reconnection mediated process may be disadvantaged due to the short time scales pertaining and a more simple process may in fact be dominant, such as direct plasma penetration via the large gyroradius (Luhmann et al., 1998).

With regard to dayside reconnection, the solar wind plasma is expected to act more strongly than in the Earth's case so that a higher incidence of reconnection is expected. This makes Mercury's magnetosphere more dynamic than that of the Earth, thereby influencing, for instance, magnetopause conditions and the transport of energy from the dayside to the nightside. The relationship between the solar wind as a driver and dayside reconnection can be studied with MGF and MPPE (on board MMO) and with MAG and SERENA (on board MPO).

Tail reconnection is considered to be the driver of substorm disturbances and, in this regard, there are distinctive characteristics of the Hermean magnetosphere, which need to be taken into account. These include: (1) its weak exo-ionosphere that may not supply sufficient plasma to the tail during storms, (2) the contribution of a high reconnection rate and (3) asymmetric current sheets. Asymmetry of the current sheets is more easily realised at Mercury because of the dominance of the IMF-B_x component. Multi-point observations of magnetic fields and plasma fluxes are essential in studying the geometry and properties of tail reconnection at Mercury.

4.3.3. Waves

The physics of ULF waves at Mercury is believed to be different from the terrestrial case. The eigenfrequency of the dipolar magnetic field is of the order of the ion gyro-frequency at Mercury (Glassmeier et al., 2003, 2004). It is suggested that a dawn–dusk asymmetry of the Kelvin–Helmholtz instability exists at the magnetopause of Mercury and this should result in an asymmetry in ULF wave activity (Glassmeier and Espley, 2006). Potential direct exposure of the planet's surface to the solar wind plasma causes us to expect the non-negligible presence of heavy ions in the magnetosphere, which may easily assume a distribution function shape (ring etc.) that excites low-frequency waves. The two BC spacecrafts are capable of investigating the spatial properties of such ULF waves.

The plasma sheet of a small magnetosphere is vulnerable to the destabilising effects of waves (such as lower-hybrid waves at the current sheet boundary). It is expected that there will be far more opportunities at Mercury than at Earth for studying current sheet dynamics. One may even question if the Hermean current sheet can become stable at all. Electron observations by MPPE–MEA, together with wave observations around the LHD frequency by PWI, will be important in addressing this issue. MPO in the near-tail will allow the large-scale consequences of current sheet dynamics driven by local electron-scale dynamics to be simultaneously monitored.

4.3.4. Magnetosphere–exo-ionosphere coupling

One of the more intriguing tasks of the BC mission related to Mercury's environment is the identification and characterisation of its exo-ionosphere and the investigation of the current system in the Hermean magnetosphere.

Taking cognisance of those large temporal variations in less than 24 h of planetary ions sources suggested by ground-based observations (e.g. Potter et al., 1999), simultaneous particle observations of MPO and MMO will be important. The close-to-planet observations of SERENA-PICAM will provide the composition and velocity distribution of planetary ions. Electron and ion-phase space densities by MPPE-HEP-e and MEA can be obtained at different distances from the planet.

Complementary measurements of magnetic fields at the two vantage points of MAG and MGF and of the electric fields (PWI) will help in elucidating the scenario of particle dynamics and currents.

4.3.5. Auroral processes

Solar wind and exospheric ion precipitation patterns largely depend on magnetospheric convection, and are controlled not only by solar wind conditions but also by surface conductivity. Hence, observations of plasma flow aboard the two spacecraft (by MPO/SERENA–MIPA and PICAM and by MMO/MPPE–MEA and MIA and PWI DC electric field experiments) will provide important information about the magnetosphere–surface interaction.

In circumstances where MMO is located in the solar wind and MPO in the dayside magnetosphere (Fig. 6, centre panel), it will be possible to investigate the planetary response to solar wind conditions. More specifically, joint measurements of MPPE–MEA and MIA, MGF and PWI, on the MMO spacecraft and SIXS, SERENA–MIPA and PICAM and MAG on the MPO spacecraft, will confirm plasma penetration inside the magnetosphere. Simultaneously, MIXS will observe the X-ray emission of planetary aurorae while SERENA–ELENA will monitor the emission of neutral atoms together with MPPE–ENA (Fig. 7). In this way, a kind of mapping of plasma precipitation at different energies will be obtained. SERENA–STROFIO and PHEBUS will observe the exospheric response of Mercury in terms of column density, composition and profile variations.

4.3.6. Extreme events at Mercury

The study of the reaction of Mercury to extreme solar wind conditions (e.g. shocks, coronal mass ejections) and solar energetic particle (SEP) arrivals is particularly interesting since, in this case, the whole planetary dayside could be involved in the response. In particular, when an

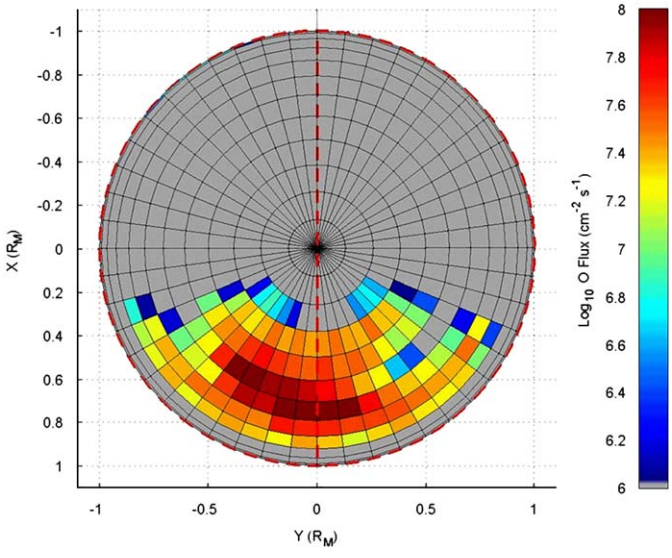

Fig. 7. Polar map of oxygen ion sputtering/escape from the surface of Mercury. The size of the emitting areas is strongly dependent on the pertaining solar wind properties (from Mura et al., 2006).

SEP event impacts Mercury, a significantly enhanced flux of energetic particles will reach the surface. According to their energies, SEPs can produce secondary particles (by interaction with the soil) and contribute to planetary X-ray fluorescence and even to exospheric changes (e.g. Potter et al., 1999; Leblanc and Johnson, 2003).

Extreme conditions refer to solar wind velocities of the order of 1000 km/s and a density that is several times higher than under normal conditions. A 3D, kinematic, solar wind model (Hakamada-Akasofu-Fry version 2/HAFv.2; McKenna-Lawlor et al., 2006; Fry et al., 2007) was already used to predict interplanetary shock arrivals at Venus, Earth and Mars following a sequence of significant solar events in December 2006 and these predictions were successfully validated using in situ measurements (McKenna-Lawlor et al., 2008). It is foreseen that the same technique will be used to predict shock arrivals at Mercury.

Fig. 8 shows the simulated impact flux of H^+ ions on the surface of Mercury under extreme conditions employing a quasi-neutral-hybrid model (McKenna-Lawlor et al., 2007; see also Kallio and Janhunen, 2003a). In these circumstances, magnetosheath plasma is pushed very close to the surface of Mercury near the sub-solar point. The impacting particles depicted ($2.67 \times 10^{27}\,s^{-1}$), correspond to about 38% of the H^+ ions that would pass through a disc of radius $r = 2440$ km in the solar wind under the extreme conditions of solar wind velocity and density considered. The conductivity of the planet and temporal variations in the solar wind affect the strength of the induced magnetic field and can consequently induce electric currents within Mercury's surface (Janhunen and Kallio, 2004).

As far as SEPs are concerned, their intensity and energy spectra vary significantly from event to event (e.g. Reames, 1999); hence, to simulate the propagation of SEPs in Mercury's magnetosphere and their interaction with the planetary surface, computations of the characteristic parameters of individual SEP events (e.g. spectra, fluence, maximum flux) at Mercury's orbit are required. Then, the SEP flux reaching the surface, the motion of charged particles inside the magnetosphere, as well as the flux of particles backscattered from the surface will each be determined on an ongoing basis during the BC mission by MPO/SIXS, MPO/SERENA and MMO/MPPE.

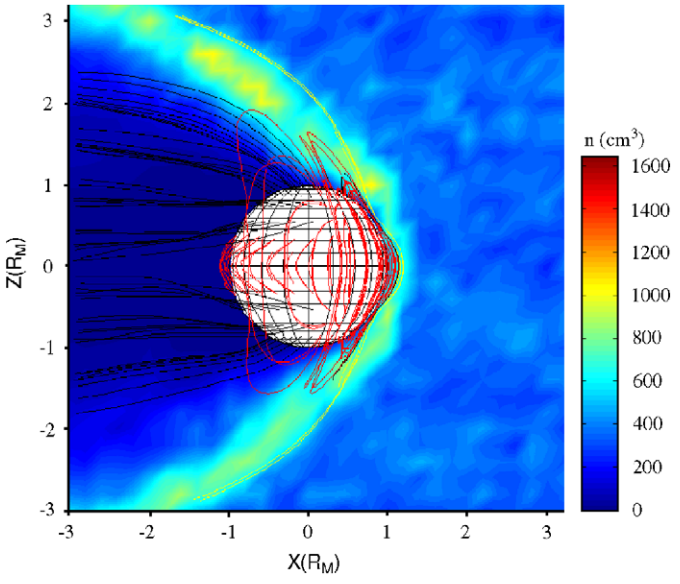

Fig. 8. Simulated impact flux of H^+ ions on the surface of Mercury. Inputs are: velocity 1000 km/s, density 380 cm^{-3} and IMF: 0, 0, and 10 nT (McKenna-Lawlor et al., 2007).

Since extreme events are very dynamic and transient, it will be important to trigger dedicated observations of such phenomena through using a forecasting model to predict solar wind macrostructure or SEP arrivals. In this regard, direct relatively short-term observations of SEPs from the Sun can be obtained by MPO/SIXS in the solar wind as well as inside the magnetosphere, since the SEP trajectories are negligibly modified by the internal magnetic field of Mercury. Hence, MPO/SIXS data can provide the opportunity to have a useful, near-real-time, forecast of solar activity that could be used to alert instruments, such as MPO/SERENA, MPO/MIXS and MPO/PHEBUS (which aim to evaluate the planet's response to solar disturbances) so that they are commanded to function in appropriate observing modes.

4.3.7. *Neutral atoms–ion coupling (charge-exchange)*

The plasma circulating inside Mercury's magnetosphere could interact with exospheric atoms via charge-exchange, hence producing hydrogen-energetic neutral atom (ENA) signals in an energy range from several hundreds of eV to tens of keV (Mura et al., 2006). This kind of plasma remote sensing, already successfully accomplished in many planetary environments (see reviews by Mitchell et al., 2000; Krimigis et al., 2004; Barabash et al., 2006; Orsini et al., 2008a), will provide information about global plasma circulation. The time scale of the emission of such signals is the same as that of corresponding magnetospheric variations (i.e. a few minutes at Mercury). Hence the ENA signal would be seen as localised bursts. On the basis of solar wind entry through the cusps and circulation inside the magnetosphere, Mura et al. (2006) predicted strong ENA emissions (10^5–$10^6\,cm^2\,s\,sr^{-1}$) from the morning side of the planet toward dawn and nightside; the signal intensity will be a maximum when the line of sight is directed tangentially to the planet since the integrated column would then be longer and also because the bulk of the neutral atmosphere is located rather close to the surface.

A global-scale MPPE–ENA instrument located on the BC/MMO will study the solar wind–exosphere interactions. These investigations will be complemented by SERENA–ELENA when MPO is close to the nightside or to the dawnside apoherm (Mura et al., 2006). The two instruments will detect ENAs using different FOVs, and different angular and energy resolution. Thus, a combined analysis of these data will provide fruitful, complementary

information. ENA detection from two vantage points is particularly important to allow an appropriate deconvolution of the signal to reconstruct the parent ion populations (e.g. DeMajistre et al., 2004).

4.4. Exospheric observations in the remote sensing of surface properties

Mercury's exposed surface is probably composed of a variety of constituents, including meteoritic and cometary materials and interplanetary dust, as well as substances originating in the planet's bulk (Hapke, 2001). The relative importance of these two types of material is not known at present. On the basis of existing models, the fraction of meteoritic material is estimated to be within the range 5–20% to 100% (Bentley et al., 2005) (with virtually no release of regolith erosion products in the latter case). According to another hypothesis, the composition of the Hermean exosphere reflects the chemical composition of impacting meteorites, possibly mixed with solar wind products, and no genetic link between the regolith and the exosphere exists (Koehn and Sprague, 2007). If only a small fraction of Mercury's exosphere is of meteoritic origin, the remainder comes from the regolith, or more precisely from an upper layer, in equilibrium with the exosphere (Killen et al., 2004). Probably, the composition of this upper superficial layer, eroded by energetic particles and radiation fluxes, significantly differs from the composition of non-eroded deeper layers due to the different extraction rates of species of various natures that are, further, subject to a variety of extraction mechanisms (Leblanc and Johnson, 2003). In a steady state, the net escape of fluxes of species at the top of the exosphere must be equal to the net fluxes extracted at the surface, thus reflecting the chemical composition of the unperturbed subjacent regolith. Therefore, the composition of the bulk regolith could be better derived using the total escape rates of atoms and ions (balanced between inflow and outflow in the planet's environment) than from a study of the surface itself (Leblanc et al., 2007).

Due to the strong link between the exosphere and the surface, it is possible by measuring neutrals and ions at relatively low altitudes to obtain information regarding the composition of the upper surface of the regolith. However, some release processes are non-stoichiometric and involve only selected species. For example, thermal evaporation and photo-stimulated desorption are more effective for volatiles (like H, He, Na, K, S, Ar, H_2O), if present on the surface. Conversely, ion-sputtering (Killen et al., 2001; Wurz and Lammer, 2003; Lammer et al., 2003) and impact vaporisation (Cintala, 1992; Gerasimov et al., 1998; Cremonese et al., 2005, 2006) are relatively stoichiometric in releasing species from the surface (adding O, Ca, Mg, Si and other refractory species to the previous list). The release efficiencies for these more stoichiometric processes depend on mineralogy (i.e. on the binding energy of the released atoms) and their altitude profiles depend on the mass and initial velocity distribution of each concerned species. Particles can be released from the surface in molecular form and then dissociated by solar radiation or by energetic ions. For instance, the high temperature observed in the Ca line has been explained by dissociation of the CaO molecule after it is released from the surface (Killen et al., 2005). Furthermore, the lifetime for H_2O dissociation is 8×10^4 s at 1 AU. Hence, probably only dissociation products such as H and OH will be detectable in Mercury's exosphere. Therefore, to be able to successfully infer the source composition from exospheric measurements, it is really important to know the mechanism of ejection and the properties of the particular emitting surface. Then, taking into account the effectiveness of that process in releasing material, information regarding the surface composition can be deduced. Conversely, if we know the upper surface composition then, by observing exospheric composition and altitude profiles, information concerning active release process can be derived (Wurz et al., 2007).

From the above considerations, it follows that the processes that will provide increased information regarding the surface composition are ion-sputtering and micrometeoroid or meteoroid impact vaporisation since these mechanisms release the majority of surface species.

4.4.1. Plasma–surface interaction

Neutrals released via the ion-sputtering process can be discriminated from neutrals produced by other mechanisms based on their specific characteristics. As already mentioned, this process stimulates highly localised and dynamic particle release. Furthermore, it is characterised by the presence of refractory species and of particles exhibiting a wide energy range (Lammer et al., 2003).

Exospheric neutral atoms at thermal energies will be detected in situ by the mass spectrometer SERENA–STROFIO while the corresponding column density profile will be determined by the UV spectrometer PHEBUS. The Na density profile will, meanwhile, be observed from a different vantage point by MMO/MSASI. The signature of ion-sputtering would be a sudden or not recurrent increase of exospheric density especially for refractory elements, while, at the same time, MPO/SERENA-ELENA and MMO/MPPE-ENA will detect neutral atoms at higher energies, correlated with an ion flux to the surface seen by MPO/SERENA-MIPA or MMO/MPPE. Thus, it will be possible to identify neutral atoms generated by the ion-sputtering process and to map their sites of generation on the surface. A comparative analysis of these measurements will allow evaluation of the composition of particles released from the upper surface. Furthermore, BC will offer for the first time an opportunity to evaluate the efficiency of the regolith in ejecting material when impacted by ions from interplanetary space. This will be achieved via coordinated measurements that will permit the correlation of neutral fluxes with simultaneous

observations of plasma precipitation using the MPO ion sensors of SERENA. If both spacecraft are inside the same flux tube (as could be the case during the closest approach scenario shown in Fig. 5c), it will be possible to inter-compare data measured by the MMO/MPPE sensors with magnetic field measurements obtained by MAG and MGF. In such a case, the possibility to trace particle trajectories with high accuracy will permit the construction of the relevant ion precipitation map in terms of flux and energy. Such an inflow map, when compared with the escaping neutral atom map obtained by ELENA, would permit the determination of surface ejection efficiency. The surface elemental abundances mapped by MIXS, the surface mineralogy mapped by MERTIS and the surface-cratering mapped by SYMBIO-SIS will allow released exospheric atoms to be related to the constitution of the surface.

4.4.2. *Meteoroids and dust on the surface*

Micrometeoroid impact vaporisation is expected to be the most efficient process on the nightside and, indeed, this is the only process that is constantly active over the whole surface of the planet (Killen et al., 2001; Wurz and Lammer, 2003). Other generally more effective processes, such as ion- and photo-stimulated desorption and thermal desorption, are mainly active in specific regions of the dayside. The detection of refractories and molecules in a low-energy range by STROFIO at spacecraft altitudes and/or by PHEBUS above 200 km in combination with zero-signal detection by ELENA at higher energies could be a signature of micrometeoroid impact vaporisation, provided that these instruments observe the same region. The MDM sensor will provide information concerning the dust distribution at Mercury and this could help in evaluating the efficiency of the release process.

Recently, Mangano et al. (2007) demonstrated that individual impact vaporisation events on Mercury involving large meteoroids (about 10 cm or more in radius) have a high probability (close to 1 after 1 month during the BepiColombo mission) to be observed as temporal elemental enhancements in the planet's exosphere (Fig. 9). The material involved in the impact is vaporised within a volume proportional to the meteoroid mass (Cintala, 1992). Hence, the analysis of such signals, taking into account the physics of the impact process and the particle transport in the exosphere, could provide key information concerning the planetary regolith composition below the first external layers, which are highly modified by space-weathering action. In particular, in the case of large impacts, this could be the only way to obtain remote-sensing information about the endogenic deeper layers (down to some metres, depending on the density and porosity of the regolith). A comparison with the MIXS composition maps will be fruitful in validating such observations and in estimating impact locations.

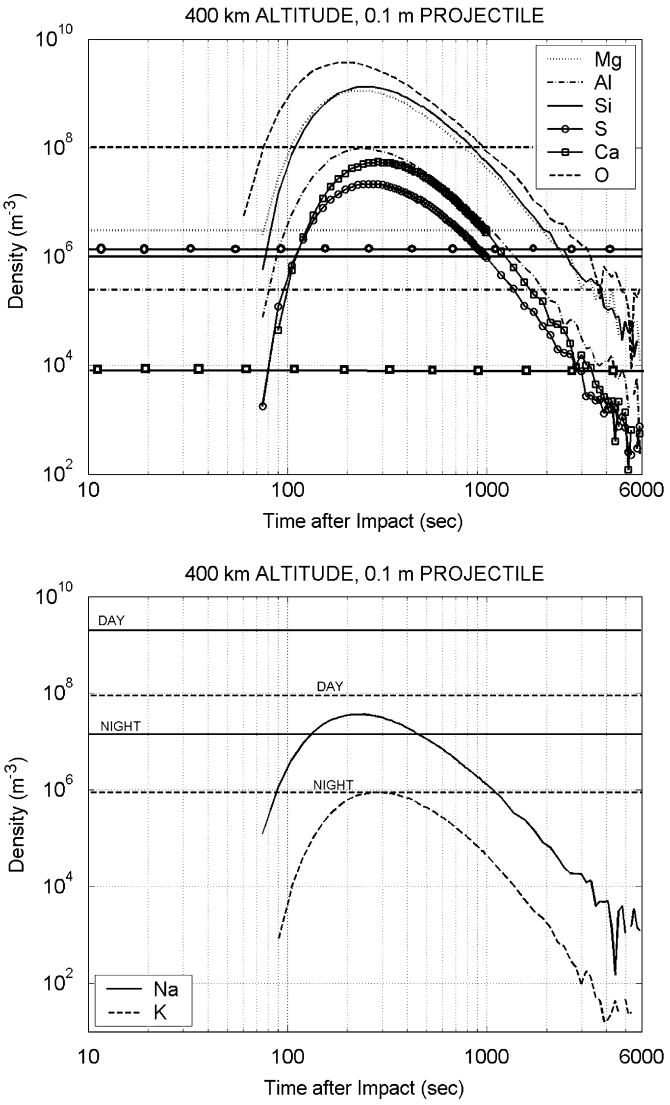

Fig. 9. Density versus time for an impacting object of 0.1 m radius at 400 km altitude for species whose mean density value does not change between day- and night-time (top), separately, for Na and K (bottom). Horizontal lines represent the exospheric background for each species according to the exospheric model of Wurz and Lammer (2003) (from Mangano et al., 2007).

5. Conclusions

The BC mission to Mercury will offer an unprecedented opportunity to investigate magnetospheric dynamics, the Hermean exosphere and the planet's interaction with solar electromagnetic radiation, the solar wind and interplanetary dust, thereby providing important insights into Mercury's evolution. Co-ordinated measurements made by different onboard instruments will enable key questions to be answered regarding the planet's environment. Furthermore, the opportunity offered by the BC mission to perform two-point simultaneous measurements provides a powerful and unique investigative tool at a location other than the Earth. Studies of dynamic magnetospheric features, such as substorms, reconnection events and

ULF waves, can be implemented by combining the observations of individual payload instruments. Moreover, the interaction of the planet with interplanetary space can be fully investigated in the case of: solar wind precipitation toward the surface, CME arrivals and meteoroid impacts. The strong coupling between different parts of the Hermean environment (magnetosphere, exo-ionosphere, exosphere and surface) makes this a locality particularly suited to mounting intercoordinated investigative programs.

The interaction processes acting at Mercury are present also in other interplanetary environments. For example, the plasma–surface interaction is present wherever a body in the Solar System lacks an atmosphere (Moon, asteroids, Jupiter's satellite Europa and many other satellites of the giant planets). Following the analysis of data from Mercury, we may gain a new way of looking at Europa and the Moon. The intrinsic magnetic field, which is rather weak but yet strong enough to sustain a magnetosphere, adds complexity to the problem, and makes comparison with observations at the Moon (which lacks a magnetic field) intriguing because of this essential difference. Again, processes like magnetospheric reconnection and wave–particle interactions are present wherever a planetary magnetosphere is formed. Since the Hermean magnetosphere occupies a unique position in the space plasma physics scenario, study of Mercury's magnetospheric processes will not only provide us with a clear picture of the magnetosphere but will also broaden our field of view of general space plasma physics. This way of investigating the Plasma Universe is needed today when plans for the next-generation of space missions to investigate the terrestrial and Jovian magnetospheres are being actively developed.

Acknowledgments

This paper is supported by the Italian Space Agency.

Appendix A. Other Hermean Environment WG members

Barabash, S. (IRF, Sweden); Benkhoff, J. (ESA, Holland); Capria, M.T. (INAF/IASF, Italy); Carpenter, J. (STAR, UK); Cassidy, T. (Virginia University., USA); (Chanteur, G. (CETP, France); Chassefiere, E. (CNRS/Service d'Aer., France); Dandouras, I. (CESR, France); Delcourt, D. (CETP, France); Fraenz, M. (MPS, Germany); Gaboriaud, A. (CNES, France); Glassmeier, K.-H. (Technische Universität Braunschweig, Germany); Grande, M. (University of Wales, UK); Hayakawa, H. (JAXA/ISAS, Japan); Hirahara (JAXA/ISAS, Japan); Ho, G. (JHUAPL, USA); Huovelin (University of Helsinki, Finland); Johnson, R. (Virginia University, USA); Kataoka, R. (STELAB, Japan); Khodachenko, M. (IWF, Austria); Killen, R.M. (Maryland University, USA); Lammer, H. (IWF, Austria); Lichtenegger, H. (IWF, Austria); Livi, S. (SWRI, Texas, USA); Mangano, V. (INAF/IFSI, Italy); Matsuoka, A. (JAXA/ISAS, Japan); Moncuquet, M. (Observatoire de Paris, France); Nilsson, H. (IRF, Sweden); Orsini, S. (INAF/IFSI, Italy); Saito (JAXA/ISAS, Japan); Sauvaud, J.-A. (CESR, France); Slavin, J.A (NASA/GSFC, Maryland, USA); Talboys, D. (University of Leicester, UK); Terada, N. (Nagoya University, Japan); Torkar, K. (IWF, Austria); Wielders, A. (ESA, Holland); Wieser, M. (IRF, Sweden); Woch, J. (MPI, Germany).

References

Barabash, S., et al., 2006. The analyzer of space plasmas and energetic atoms (ASPERA-3) for the Mars Express mission. Space Sci. Rev.

Baumjohann, W., Matsuoka, A., Glassmeier, K.-H., Russell, C.T., Nagai, T., Hoshino, M., Nakagawa, T., Balogh, A., Slavin, J.A., Nakamura, R., Magnes, W., 2006. The magnetosphere of Mercury and its solar wind environment: open issues and scientific questions. Adv. Space Res. 38, 604–609.

Baumjohann, W., et al., 2008. Magnetic field investigation of Mercury's magnetosphere and the inner heliosphere by MMO/MGF. Planet. Space Sci., doi:10.1016/j.pss.2008.05.019.

Bentley, M.S., Ball, A.J., Dyar, M.D., Pieters, C.M., Wright, I.P., Zarnecki, J.C., 2005. Space weathering: laboratory analyses and in-situ instrumentation. Lunar Planet. Sci. XXXVI.

Bida, T.A., Killen, R.M., Morgan, T.H., 2000. Discovery of calcium in Mercury's atmosphere. Nature 404, 159–161.

Blomberg, L.G., Cumnock, J.A., Glassmeier, K.-H., Treumann, R.A., 2007. Plasma waves in Hermean magnetosphere. Space Sci. Rev. 132, 575–591.

Boardsen, S.A., Slavin, J.A., 2007. Search for pick-up ion generated Na^+ cyclotron waves at Mercury. Geophys. Res. Lett. 34, L22106.

Boardsen, S.A., Anderson, B.J., Korth, H., Slavin, J.A., 2008. Ultra-low frequency wave observations by MESSENGER during its January 2008 flyby through Mercury's magnetosphere. Eos. Trans. AGU 89 (23) Jt. Assem. Suppl.

Broadfoot, A.L., Kumar, S., Belton, M.J.S., McElroy, M.B., 1974. Mercury's atmosphere from Mariner 10: preliminary results. Science 185, 166–169.

Carpenter, et al., 2008. The mercury imaging X-ray spectrometer's (MIXS's) contribution to our understanding of Mercury. Planet. Space Sci., this issue.

Chassefière, et al., 2008. PHEBUS: a double ultraviolet spectrometer to observe Mercury's exosphere. Planet. Space Sci. 56, 201–223.

Christensen, U.R., 2006. A deep dynamo generating Mercury's magnetic field. Nature 444, 1056–1058.

Christon, S.P., Feynman, J., Slavin, J.A., 1987. Dynamic substorm injections: similar magnetospheric phenomena at Earth and Mercury. In: Lui, A.T.Y. (Ed.), Magnetotail Physics. Johns Hopkins University Press, Baltimore, MD, pp. 393–400.

Cintala, M.J., 1992. Impact-induced thermal effects in the Lunar and Mercurian regoliths. J. Geophys. Res. 97, 947–973.

Connerney, J.E.P., Ness, N.F., 1988. Mercury's magnetic field and interior. In: Vilas, F., Chapman, C.R., Matthews, M.S. (Eds.), Mercury. The University of Arizona Press, Tucson, pp. 514–561.

Cowley, S.W.H., 1995. Theoretical perspectives of the magnetopause: a tutorial review, in physics of the magnetopause. AGU Geophys. Monogr. 90, 29–43.

Cowley, S.W.H., Owen, C.J., 1989. A simple illustrative model of open flux tube motion over the dayside magnetopause. Planet. Space Sci. 37, 1461–1475.

Cremonese, G., Bruno, M., Mangano, V., Marchi, S., Milillo, A., 2005. Neutral sodium atoms release from the surface of Mercury induced by meteoroid impacts. Icarus 177, 122.

Cremonese, G., Bruno, M., Mangano, V., Marchi, S., Milillo, A., 2005. Neutral sodium atoms release from the surface of Mercury induced by meteoroid impacts. Icarus 177, 122 and 2006 Corrigendum Icarus 182, 297.

Cremonese, G., et al., 2008. Techniques and methods in ground-based observation of Mercury. Planet. Space Sci. 56, 61–78.
Delcourt, D. C., Seki, K., 2006. On the dynamics of charged particles in the magnetosphere of Mercury. In: Ip, W.-H., Bhardwaj, A. (Eds.), Adv. Geosci. 3, 17.
Delcourt, D.C., Grimald, S., Leblanc, F., Berthelier, J.-J., Millilo, A., Mura, A., Orsini, S., Moore, T.E., 2003. Ann. Geophys. 21, 1723.
Delcourt, D.C., Seki, K., Terada, N., Miyoshi, M., 2005. Electron dynamics in the storm-time magnetosphere of Mercury. Ann. Geophys. 23, 3389–3398.
Delcourt, D.C., Leblanc, F., Seki, K., Terada, N., Moore, T.E., Fok, M.-C., 2007. Ion energization during substorms at Mercury. Planet. Space Sci. 55, 1502–1508.
DeMajistre, R., Roelof, E.C., son Brandt, P.C., Mitchell, D.G., 2004. Retrieval of global magnetospheric ion distributions from high-energy neutral atom measurements made by the IMAGE/HENA instrument. J. Geophys. Res. 109, A04214, 10.1029/2003JA010322.
Domingues, D.L., Koehn, P.L., Killen, R.M., Sprague, A.L., Sarantos, M., Cheng, A.F., Bradley, E.T., McClintock, W.E., 2007. Mercury's atmosphere: a surface-bounded exosphere. Space Sci. Rev. 131, 161–186.
Erickson, J.E., 1968. Velocity distribution of sporadic photographic meteors. JGR 73, 3721–3726.
Flamini, E., et al., 2008. Planet. Space Sci., this issue.
Fry, C.D., Detman, T.R., Dryer, M., Smith, Z., Sun, W., Deehr, C.S., Akasofu, S.-I., Wu, C.-C., McKenna-Lawlor, S., 2007. Real-time solar wind forecasting capabilities and challenges. J. Atmos. Solar-Terr. Phys. 69, 109–115.
Fujimoto, M., Baumjohann, W., Kabin, K., Nakamura, R., Slavin, J.A., Terada, N., Zelenyi, L., 2007. Hermean magnetosphere–solar wind interaction. Space Sci. Rev. 132, 529–550.
Fujimoto, M., Laakso, H., Benkhoff, J., 2008. Preface and Science goals of BepiColombo. Planet. Space Sci., this issue.
Gerasimov, M.V., Ivanov, B.A., Yakovlev, O.I., 1998. Physics and chemistry of impacts. Earth Moon Planet. 80 (1/3), 209–259.
Glassmeier, K.-H., 2000. Currents in Mercury's magnetosphere, magnetospheric current systems. Geophys. Monogr. 118, 371–380 AGU, Washington, DC.
Glassmeier, K.-H., Espley, J., 2006. ULF waves in planetary magnetospheres, magnetospheric ULF waves: synthesis and new directions. Geophys. Monogr. 169, 341–359 AGU, Washington, DC.
Glassmeier, K.-H., Mager, P.N., Klimushkin, D.Y., 2003. Concerning ULF pulsations in Mercury's magnetosphere. Geophys. Res. Lett. 30, 1928.
Glassmeier, K.-H., Klimushkin, D., Othmer, C., Mager, P., 2004. ULF waves at Mercury: Earth, the giants, and their little brother compared. Adv. Space Res. 33, 1875–1883.
Glassmeier, K.-H., Auster, H.-U., Motschmann, U., 2007a. A feedback dynamo generating Mercury's magnetic field. Geophys. Res. Lett. 34, L22201.
Glassmeier, K.-H., Grosser, J., Auster, U., Constantinescu, D., Narita, Y., Stellmach, S., 2007b. Electromagnetic induction effects and dynamo action in the Hermean system. Space Sci. Rev. 132, 511–527.
Glassmeier, K.-H., et al., 2008. The Fluxgate Magnetometer of the BepiColombo Mercury Planetary Orbiter. Planet. Space Sci. 56, 287–299.
Gold, R.E., et al., 2001. The MESSENGER mission to Mercury: scientific payload. Planet. Space Sci. 49, 1467–1479.
Gombosi, T.I., Dezeeuw, D.L., Groth, C.P.T., Powell, K.G., 2000. Magnetospheric configuration for Parker-spiral IMF conditions: results of A 3D AMR MHD simulation. Adv. Space. Res. 26, 139–149.
Grosser, J., Glassmeier, K.-H., Stadelmann, A., 2004. Induced magnetic field effects at planet Mercury. Planet. Space Sci. 52, 1251–1260.
Hajakawa, van Casteren, J., Ferri, 2008. Planet. Space Sci., this issue.
Hapke, B., 2001. Space weathering from Mercury to the asteroid belt. J. Geophys. Res. 106 (E5), 10039–10074.
Helbert, J., Moroz, L., Maturilli, A., Bischof, A., Warell, J., Sprague, A., Palomba, E., 2007. A set of laboratory analogue materials for the MERTIS instrument on the ESA BepiColombo mission to Mercury. Adv. Space Res.
Hiesinger, H., et al., 2008. Planet. Space Sci., this issue.
Hill, T., Dessler, A., Wolf, R., 1976. Mercury and Mars: the role of ionospheric conductivity in the acceleration of magnetospheric particles. Geophys. Res. Lett. 3 (8), 429–432.
Hunten, D.M., Sprague, A.L., 1997. Origin and character of the lunar and mercurian atmospheres. Adv. Space Res. 19 (10), 1551–1560.
Hunten, D.M., Sprague, A.L., 2002. Diurnal variation of Na and K at Mercury. Meteor. Planet. Sci 37, 1165.
Hunten, D.M., Morgan, T.M., Shemansky, D.M., 1988. The Mercury atmosphere. In: Vilas, F., Chapman, C., Matthews, M. (Eds.), Mercury. University of Arizona Press, Tucson, AZ, pp. 562–612.
Huovelin, J., et al., 2005. SIXS, the solar intensity X-ray and particle spectrometer for BepiColombo. Gephys. Res. Abstr. 7, 08003.
Ip, W.H., 1986. The sodium exosphere and magnetosphere of Mercury. Geophys. Res. Lett. 13, 423–426.
Ip, W.-H., Kopp, A., 2002. MHD simulations of the solar wind interaction with mercury. J. Geophys. Res. 107 (A11), 1348.
Janhunen, P., Kallio, E., 2004. Surface conductivity of Mercury provides current closure and may affect magnetospheric symmetry. Ann. Geophys. 22, 1829–1837.
Johnson, R.E., Quickenden, T.I., 1997. Photolysis and radiolysis of water ice on outer solar system bodies. J. Geophys. Res. 102, 10985–10996.
Kabin, K., Gombosi, T., DeZeeuw, D., Powell, K., 2000. Interaction of Mercury with the solar wind. Icarus 143, 397–406.
Kallio, E., Janhunen, P., 2003a. Modelling the solar wind interaction with Mercury by a quasineutral hybrid model. Ann. Geophys. 21 (11), 2133–2145.
Kallio, E., Janhunen, P., 2003b. Solar wind and magnetospheric ion impact on Mercury's surface. Geophys. Res. Lett. 30 (17), 1877.
Kallio, E., Janhunen, P., 2004. The response of the Hermean magnetosphere to the interplanetary magnetic field. Adv. Space Res. 33.
Kallio, E., Wurz, P., Killen, R.M., McKenna-Lawlor, S., Milillo, A., Mura, A., Massetti, S., Orsini, S., Lammer, H., Janhunen, P., Ip, W-H., 2008. On the impact of multiply charged heavy solar wind ions on the surface of Mercury, the Moon and Ceres. Planet. Space Sci. 56 (11), 1506–1516.
Kameda, S., Yoshikawa, I., Ono, J., Nozawa, H., 2007. Time variation in exospheric sodium density on Mercury. Planet. Space Sci. 55, 1509–1517.
Kameda, S., Kagitani, M., Okano, S., Yoshikawa, I., Ono, J., 2008. Observation of Mercury's sodium tail using Fabry–Perot interferometer. Adv. Space Res. 41, 1381–1385.
Kasaba, Y., et al., 2008. The Plasma Wave Investigation (PWI) onboard the BepiColombo/MMO: first measurement of electric fields, electromagnetic waves, and radio waves around Mercury. Planet. Space Sci. 56, 238–278.
Katoh, Y., Omura, Y., 2007. Computer simulation of chorus wave generation in the Earth's inner magnetosphere. Geophys. Res. Lett. 34, L03102.
Killen, R.M., Ip, W.-H., 1999. The surface-bounded atmosphere of Mercury and the Moon. Rev. Geophys. 37, 361.
Killen, R.M., Potter, A.E., Reiff, P., Sarantos, M., Jackson, B.V., Hick, P., Giles, B., 2001. Evidence for space weather at Mercury. J. Geophys. Res. 106, 20509–20525.
Killen, R.M., Sarantos, M., Potter, A.E., Reiff, P., 2004. Source rates and ion recycling rates for Na and K in Mercury's atmosphere. Icarus 171, 1–19.
Killen, R.M., Bida, T.A., Morgan, H., 2005. The calcium exosphere of Mercury. Icarus 173, 300–311.
Killen, R.M., Potter, A.E., Mura, A., Lammer, H., Cremonese, G., Wurz, P., Orsini, S., Milillo, A., Sprague, A.L., Khodachenko, M.L., Lichtenegger, H.I.M., 2008. Processes that promote and deplete the exosphere of Mercury. Space Sci. Rev. and Space Sciences Ser. ISSI Mercury 26, 249.

Kivelson, M.G., 2005. Transport and acceleration of plasma in the magnetospheres of Earth and Jupiter and expectations for Saturn. Adv. Space Res. 36 (11), 2077–2089.

Koehn, P.L., Sprague, A.L., 2007. Solar oxygen and calcium in Mercury's exosphere. Planet. Space Sci. 55 (11), 1530–1540.

Korth, H., Anderson, B.J., Acuna, M.H., Slavin, J.A., Tsyganenko, N.A., Solomon, S.C., McNutt Jr., R.L., 2004. Determination of the properties of Mercury's magnetic field by the MESSNGER mission. Planet. Space Sci. 52, 733–746.

Korth, H., Anderson, B.J., Acuna, M.H., Johnson, C.L., Purucker, M.E., Slavin, J.A., Zurbuchen, T.H., Raines, J.M., Gloeckler, G., Schriver, D., Travnicek, P., Solomon, S.C., Gold, R.E., McNutt, R.L., 2008. Toward an improved understanding of the magnetic field of Mercury: results using data from the first MESSENGER flyby. Eos Trans. AGU 89 (23) Jt. Assem. Suppl.

Krimigis, S.M., et al., 2004. Space Sci. Rev. 114, 233.

Lammer, H., Wurz, P., Patel, M.R., Killen, R., Kolb, C., Massetti, S., Orsini, S., Milillo, A., 2003. The variability of Mercury's exosphere by particle and radiation induced surface release process. Icarus 166, 238–247.

Leblanc, F., Johnson, R.E., 2003. Mercury's sodium exosphere. Icarus 164, 261–281.

Leblanc, F., Chassefière, E., Johnson, R.E., Hunten, D.M., Kallio, E., Delcourt, D.C., Killen, R.M., Luhmann, J.G., Potter, A.E., Jambon, A., Cremonese, G., Mendillo, M., Yan, N., Sprague, A.L., 2007. Mercury's exosphere: origins and relations to its magnetosphere and surface. Planet. Space Sci. 55, 1069–1092.

Luhmann, J., Russell, C., Tsyganenko, N., 1998. Disturbances in mercury's magnetosphere: are mariner 10 "substorms" simply driven? J. Geophys. Res. 103, 9113–9119.

Mangano, V., Milillo, A., Mura, A., Orsini, S., De Angelis, E., Di Lellis, A.M., Wurz, P., 2007. Impulsive meteoritic impact vaporization in the Hermean exosphere. Planet. Space Sci. 55, 1541–1556.

Margot, J.L., Peale, S.J., Jurgens, R.F., Slade, M.A., Holin, I.V., 2007. Large longitude libration of Mercury reveals a molten core. Science 316, 710.

Massetti, S., Orsini, S., Milillo, A., Mura, A., De Angelis, E., Lammer, H., Wurz, P., 2003. Mapping of the cusp plasma precipitation on the surface of Mercury. Icarus 166/2, 229–237.

Massetti, S., Orsini, S., De Angelis, E., Mangano, V., Milillo, A., Mura, A., 2006. The dayside magnetosphere of Mercury. In: Ip, W.-H., Bhardwaj, A. (Eds.), Advances in Geosciences, A 5-volume set, vol. 3. Planetary Science (PS), pp. 29–36.

Massetti, S., Orsini, S., Milillo, A., Mura, A., 2007. Modelling Mercury's magnetosphere and plasma entry through the dayside magnetopause. Planet. Space Sci. 55, 1557–1568, 10.1016/j.pss.2006.12.008.

McClintock, W.E., Bradley, E.T., Vervack Jr., R.J., Killen, R.M., Sprague, A.L., Izenberg, N.R., Solomon, S.C., 2008. Mercury's exosphere: observations during MESSENGER's first mercury flyby. Science 321, 92.

McGrath, M.A., Johnson, R.E., Lanzerotti, L.J., 1986. Sputtering of sodium on the planet Mercury. Nature 323, 694.

McKenna-Lawlor, S., Dryer, M., Kartalev, M.D., Smith, Z., Fry, C.D., Sun, W., Deehr, C.S., Kecskemety, K., Kudela, K., 2006. Near real-time predictions of the arrival at the Earth of flare-generated shocks during solar cycle 23. J. Geophys. Res. 111, A11103.

McKenna-Lawlor, S., Kallio, E., Lammer, H., Schmidt, W., Janhunen, P., 2007. Modeled solar wind and magnetospheric ion impact on Mercury's surface in response to elevated prolonged, solar activity in December, 2006. Presentation EGU2007-A-01754 at the European Geophysical Union Meeting, Vienna.

McKenna-Lawlor, S., Dryer, M., Fry, C.D., Smith, Z.K., Intriligator, D.S., Courtney, W.R., Deehr, C.S., Sun, W., Kecskemety, K., Kudela, K., Balaz, J., Barabash, S., Futaana, Y., Yamauchi, M., Lundin, R., 2008. Predicting interplanetary shock arrivals at Earth, Mars, and Venus: a real-time modelling experiment following the flares of 5–14, December, 2006. J. Geophys. Res. 113.

Milillo, A., Orsini, S., Wurz, P., Delcourt, D., Kallio, E., Killen, R.M., Lammer, H., Massetti, S., Mura, A., Barabash, S., Cremonese, G., Daglis, I.A., De Angelis, E., Di Lellis, A.M., Livi, S., Mangano, V., Torkar, K., 2005. Surface–exosphere–magnetosphere system of Mercury. Space Sci. Rev. 117 (3), 397–444.

Mitchell, D.G., et al., 2000. Space Sci. Rev. 91, 67–112.

Morgan, T.H., Zook, H.A., Potter, A.E., 1988. Impact-driven supply of sodium and potassium to the atmosphere of Mercury. Icarus 75, 156–170.

Mura, A., Orsini, S., Milillo, A., Delcourt, D., Massetti, S., De Angelis, E., 2005. Dayside H^+ circulation at Mercury and neutral particle emission. Icarus 175, 305–319.

Mura, A., Orsini, S., Milillo, A., Delcourt, D., Di Lellis, A.M., De Angelis, E., Massetti, S., 2006. Neutral atom emission from Mercury. In: Ip, W.-H., Bhardwaj, A. (Eds.), Advances in Geoscience, vol. 3, pp. 37–50.

Mura, A., Milillo, A., Orsini, S., Massetti, S., 2007. Numerical and analytical model of Mercury's exosphere: dependence on surface and external conditions. Planet. Space Sci., 1569–1583.

Mura, A., Wurz, P., Lichtenegger, H.I.M., Schleicher, H., Lammer, H., Delcourt, D., Milillo, A., Orsini, S., Massetti, S., Khodachenko, M.L., 2008. The sodium exosphere of Mercury: comparison between observations during Mercury's transit and model results. Icarus, in press, doi:10.1016/j.icarus.2008.11.014.

Omura, Y., Furuya, N., Summers, D., 2007. Relativistic turning acceleration of resonant electrons by coherent whistler mode waves in a dipole magnetic field. J. Geophys. Res. 112, A06236.

Orsini, S., Milillo, A., Mura, A., De Angelis, E., Massetti, S., Di Lellis, A.M., 2008a. Prospects of solar system environment observations by means of ENA detection. Adv. Geosci., in press.

Orsini, S., Livi, S., Torkar, K., Barabash, S., Milillo, A., Wurz, P., Di Lellis, A.M., Kallio, E., the SERENA team, 2008b. SERENA: a suite of four instruments (ELENA, STROFIO, PICAM and MIPA) on board BepiColombo-MPO for particle detection in the Hermean Environment. Planet. Space Sci. 56, 166–181.

Potter, A.E., 1995. Chemical sputtering could produce sodium vapor and ice on Mercury. Geophys. Res. Lett. 22, 3289–3292.

Potter, A.E., Morgan, T.H., 1985. Discovery of sodium in the atmosphere of Mercury. Science 229, 651–653.

Potter, A.E., Morgan, T.H., 1986. Potassium in the atmosphere of Mercury. Icarus 67, 336–340.

Potter, A.E., Morgan, T.H., 1990. Evidence for magnetospheric effects on the sodium atmosphere of Mercury. Science 248, 835.

Potter, A.E., Morgan, T.H., 1997. Evidence for suprathermal sodium on Mercury. Adv. Space Res. 19, 1571–1576.

Potter, A.E., Killen, R.M., Morgan, T.H., 1999. Rapid changes in the sodium exosphere of Mercury. Planet. Space Sci. 47, 1441–1448.

Potter, A.E., Killen, R.M., Morgan, T.H., 2002. The sodium tail of Mercury. Meteor. Planet. Sci. 37, 1165–1172.

Potter, A.E., Killen, R.M., Sarantos, M., 2006. Spatial distribution of sodium on Mercury. Icarus 181, 1–12.

Reames, D.V., 1999. Particle acceleration at the Sun and in the heliosphere. Space Sci. Rev. 90, 413–491.

Russell, C.T., 1989. ULF waves in the Mercury magnetosphere. Geophys. Res. Lett. 16, 1253–1256.

Russell, C.T., Baker, D.N., Slavin, J.A., 1988. The magnetosphere of Mercury. In: Vilas, F., Chapman, C.R., Matthews, M.S. (Eds.), Mercury. The University of Arizona Press, Tucson, pp. 514–561.

Saito, Y., Sauvaud, J.A., Hirahara, M., Barabash, S., Delcourt, D., Takashima, T., Asamura, K., BepiColombo MMO/MPPE Team, 2008. Scientific objectives and instrumentation of Mercury Plasma Particle Experiment (MPPE) onboard MMO. Planet. Space Sci. 56, 182–200.

Santo, A.G., et al., 2001. The MESSENGER mission to Mercury: spacecraft and mission design. Planet. Space Sci. 49, 1481–1500.

Sarantos, M., Reiff, P.H., Hill, T.W., Killen, R.M., Urquhart, A.L., 2001. A Bx-interconnected magnetosphere model for Mercury. Planet. Space Sci. 49, 1629.

Sarantos, M., Killen, R.M., Kim, D., 2007. Predicting the long-term solar wind ion-sputtering source at Mercury. Planet. Space Sci. 55, 1584–1595.

Schleicher, H., Wiedemann, G., Wohl, H., Berkefeld, T., Soltau, D., 2004. Detection of neutral sodium above Mercury during the transit on 2003 May 7. Astron. Astrophys. 425, 1119–1124.

Schulz, R., 2006. BepiColombo payload and mission updates. Adv. Space Res. 38, 572–577.

Scuffham, J., Balogh, A., 2006. A new model of Mercury's magnetospheric magnetic field. Adv. Space. Res. 38, 616–626.

Sieveka, E.M., Johnson, R.E., 1984. Ejection of atoms and molecules from Io by plasma-ion impact. Astrophys. J. 287, 418–426.

Sigmund, P., 1969. Theory of sputtering. I. Sputtering yield of amorphous and polycrystalline targets. Phys. Rev. 184, 383–416.

Siscoe, G.L., Ness, N.F., Yeates, C.M., 1975. Substorms on Mercury. J. Geophys. Res. 80, 4359–4363.

Slavin, J.A., 2004. Mercury's magnetosphere. Adv. Space Res. 33, 1859–1874.

Slavin, J., Holzer, R., 1979. The effect of erosion on the solar wind standoff distance at Mercury. J. Geophys. Res. 84, 2076–2082.

Slavin, J.A., Owen, J.C.J., Connerney, J.E.P., Christon, S.P., 1997. Mariner 10 observations of field-aligned currents at Mercury. Planet. Space Sci. 45 (1), 133–141.

Slavin, J.A., Krimigis, S.M., Acuña, M.H., Anderson, B.J., Baker, D.N., Koehn, P.L., Korth, H., Livi, S., Mauk, B.H., Solomon, S.C., Zurbuchen, T.H., 2007. MESSENGER: exploring Mercury's magnetosphere. Space Sci. Rev. 131, 133–160.

Slavin, J.A., Acuna, M.H., Anderson, B.J., Baker, D.N., Benna, M., Gloeckler, G., Gold, R.E., Ho, G.C., Killen, R.M., Korth, H., Krimigis, S.M., McNutt Jr., R.L., Nittler, L., Raines, J.M., Schriver, D., Solomon, S.C., Starr, R.D., Trávníček, P., Zurbuchen, T.H., 2008. Mercury's magnetosphere after MESSENGER's first flyby. Science 321, 85.

Smyth, W.H., Marconi, M.L., 1995. Theoretical overview and modelling of the sodium and potassium atmospheres of Mercury. Astrophys. J. 441, 839–864.

Solomon, S.C., et al., 2001. The MESSENGER mission to Mercury: scientific objectives and implementation. Planet. Space Sci. 49, 1445–1465.

Solomon, S.C., McNutt Jr., R.L., Gold, R.E., Domingue, D.L., 2007. MESSENGER mission overview. Space Sci. Rev. 131, 3–39.

Southworth, R.B., Sekanina, Z., 1973. Physical and dynamical studies of meteors. NASA Contract Rep. CR-2316, 108.

Sprague, A.L., 1992. Mercury's atmospheric sodium bright spots and potassium variations: a possible cause. J. Geophys. Res. 97, 18,257–18,264.

Sprague, A.L., Massey, S.S., 2007. Mercury's exosphere: a possible source for Na. Planet. Space Sci. 55, 1614–1621.

Sprague, A.L., Kozlowski, R.W.H., Hunten, D.M., 1990. Caloris Basin: an enhanced source for potassium in Mercury's atmosphere. Science 249, 1140–1143.

Sprague, A.L., Kozlowski, R.W.H., Hunten, D.M., Schneider, N.M., Domingue, D.L., Wells, W.K., Schmitt, W., Fink, U., 1997. Distribution and abundance of sodium in mercury's atmosphere, 1985–1988. Icarus 129, 506–527.

Sprague, A.L., Schmitt, W.J., Hill, R.E., 1998. Mercury: sodium atmospheric enhancements, radar-bright spots, and visible surface features. Icarus 136, 60–68.

Spreiter, J.R., Summers, A.L., Alksne, A.Y., 1966. Hydromagnetic flow around the magnetosphere. Planet. Space Sci. 14, 223–253.

Stanley, S., Bloxham, J., Hutchison, W.E., Zuber, M.T., 2004. Thin shell dynamo models consistent with Mercury's weak observed magnetic field. Earth Planet. Sci. Lett. 234, 27–38.

Summers, D., Omura, Y., 2007. Ultra-relativistic acceleration of electrons in planetary magnetospheres. Geophys. Res. Lett. 34, L24205, doi:10.1029/2007GL032226.

Trávníček, P., Hellinger, P., Schriver, D., 2007. Structure of Mercury's magnetosphere for different pressure of the solar wind: three dimensional hybrid simulations. Geophys. Res. Lett. 34, L05104.

Tsyganenko, N.A., 1995. Modeling the Earth's magnetosperic magnetic field confined within a realistic magnetopause. J. Geophys. Res. 100, 5599–5612.

Vainio, R., for the SIXSP Team, 2005. Energetic charged particle measurements by SIXS on-board BepiColombo MPO. Gephys. Res. Abstr. 7, 06714.

Vilas, F., Chapman, C.R., Matthews, M.S. (Eds.), 1998. Mercury. University of Arizona Press, Tucson.

Wurz, P., Blomberg, L., 2001. Particle populations in Mercury's magnetosphere. Planet. Space Sci. 14–15 (49), 1643–1653.

Wurz, P., Lammer, H., 2003. Monte-Carlo simulation of Mercury's exosphere. Icarus 164 (1), 1–13.

Wurz, P., Rohner, U., Whitby, J.A., Kolb, C., Lammer, H., Dobnikar, P., Martín-Fernández, J.A., 2007. The lunar exosphere: the sputtering contribution. Icarus 191, 486–496.

Yoshikawa, I., et al., 2008. The Mercury Sodium Atmospheric Spectral Imager for the MMO Spacecraft of BepiColombo. Planet. Space Sci. 56, 224–237.

Zook, H., 1975. Hyperbolic cosmic dust: its origin and its astrophysical significance. Planet. Space Sci. 23, 183–203.

Zurbuchen, T.H., Raines, J.M., Gloeckler, G., Krimigis, S.M., Slavin, J.A., Koehn, P., Killen, R.M., Sprague, A.L., McNutt Jr., R.L., Solomon, S.C., 2008. MESSENGER observations of the composition of Mercury's ionized exosphere and plasma environment. Science 321, 90.